ANKARA YILDIRIM BEYAZIT UNIVERSITY

GRADUATE SCHOOL OF NATURAL AND APPLIED SCIENCES

DUAL-POLARIZED H-SHAPED APERTURE-COUPLED MICROSTRIP ANTENNA FOR SUB-6GHZ 5G COMMUNICATION SYSTEMS

M.Sc. Thesis by

Bashar Khayal

Department of Electrical and Electronics Engineering

December 2022

ANKARA

DUAL-POLARIZED H-SHAPED APERTURE-COUPLED MICROSTRIP ANTENNA FOR SUB-6GHZ 5G COMMUNICATION SYSTEMS

A Thesis Submitted to

The Graduate School of Natural and Applied Sciences of

Ankara Yıldırım Beyazıt University

In Partial Fulfillment of the Requirements for the Degree of Master of Science in Electrical and Electronics Engineering, Department of Electrical and Electronics Engineering

By

Bashar Khayal

December 2022

ANKARA

M.Sc. THESIS EXAMINATION RESULT FORM

We have read the thesis entitled **" DUAL-POLARIZED H-SHAPED APERTURE-COUPLED MICROSTRIP ANTENNA FOR SUB-6GHZ 5G COMMUNICATION SYSTEMS "** completed by: **BASHAR KHAYAL** under the supervision of **Prof. Dr. ALAADEEN ELROUBY** and we certify that in our opinion it is fully adequate, in scope and in quality, as a thesis for the degree of Master of Science.

Prof. Dr. ALAAELDEEN ELROUBY

Supervisor

Prof. Dr. HÜSEYİN CANBOLAT

Jury member

Prof. Dr. MEHMET ÜNLÜ

Jury Member

Prof. Dr. Sadettin ORHAN

Director
Graduate School of Natural and Applied Sciences

ETHICAL DECLARATION

I hereby declare that, in this thesis which has been prepared in accordance with the Thesis Writing Manual of Graduate School of Natural and Applied Sciences,

- All data, information, and documents are obtained in the framework of academic and ethical rules,
- All information, documents, and assessments are presented in accordance with scientific ethics and morals,
- All the materials that have been utilized are fully cited and referenced,
- No change has been made of the utilized materials,
- All the works presented are original,

and in any contrary case of above statements, I accept to renounce all my legal rights.

Date: 20/12/2022 **Signature:……...**

Name & Surname: Bashar Khayal

ACKNOWLEDGMENTS

First and above all, I would like to thank the almighty Allah for bestowing his blessings on me and offering me the strength to carry out and complete this work.

I am extremely grateful to Prof. Dr. ALAAELDEEN ELROUBY, my superiors, for his valuable advice, guidance, helpful discussions, and motivation during my study. Apart from his helpful academic advice and encouragement, he was extremely kind, polite, and supportive. I am also very grateful to the members of my thesis committee, Prof. Dr. HÜSEYİN CANBOLAT and Prof. Dr MEHMET ÜNLÜ for their consideration, support, and helpful advice.

I would like to express my special thanks to my parents, my brothers and my sister for their encouragement, patience, and love. It would have been impossible for me to complete this work without their support, inspiration and understanding. Finally, my heartfelt gratitude to all those who helped me in completing this work.

2022, 20 December **Bashar Khayal**

DUAL-POLARIZED H-SHAPED APERTURE-COUPLED MICROSTRIP ANTENNA FOR SUB-6GHZ 5G COMMUNICATION SYSTEMS

ABSTRACT

The 5G wireless communication technology is seen as a big change in the business of wireless communication, where 5G is the major phase beyond the current 4G. This rapid revolution motivates researchers to advance communication technologies in software and hardware areas. The performance of radio communications in any wireless device depends on the design of an efficient antenna. So, this thesis presents single element and arrays at 3.5 GHz for microstrip antennas. Where 3.5GHz is the center frequency of the N78 sub-6GHz 5G frequency band.

A broadband dual-polarized aperture-coupled microstrip antenna is designed and presented. Aperture-coupled feeding technique is considered to achieve the broadband characteristic. An H-shaped slot is considered, which provides the broadband with a shorter slot length.

Based on the best optimized single element, several dual-polarized microstrip antenna arrays are designed in order to enhance the realized gain of the antenna design to meet the 5G specifications. Commercial simulation Studio Suite (CST) and Advanced Design System (ADS) were used to design the single element and planar arrays.

Parallel feed techniques were utilized to feed the antenna array providing good antenna performance, which can be used in sub-6GHz 5G handset mobiles and base station systems.

Keywords: Dual-polarized, Aperture-coupled, H-shaped, Microstrip antenna, Antenna array, Sub-6GHz, 5G communication**.**

SUB-6GHZ 5G HABERLEŞME SİSTEMLERİ İÇİN ÇİFT POLARİZE H-ŞEKİLLİ AÇIKLIK-KUPLELI MİKROŞERİT ANTEN

ÖZ

5G iletişim teknolojisi, 5G'nin mevcut 4G'nin ötesindeki ana aşama olduğu kablosuz iletişim işinde bir devrim olarak kabul edilir. Bu hızlı devrim, araştırmacıları yazılım ve donanım alanlarında iletişim teknolojilerini geliştirmeye motive ediyor. Herhangi bir kablosuz cihazda radyo iletişiminin performansı, verimli bir anten tasarımına bağlıdır. Dolayısıyla bu tez, mikroşerit antenler için 3.5 GHz'de tek eleman ve diziler sunmaktadır. 3.5GHz, N78 alt-6GHz 5G frekans bandının merkez frekansıdır.

Geniş bantlı çift kutuplu bir mikroşerit anten tasarlanmış ve ölçülmüştür. Geniş bant karakteristiğini elde etmek için açıklığa bağlı mikroşerit anten düşünülmüştür. Geniş bant için daha kısa bir yuva uzunluğu sağlayan H-şekilli bir yuva düşünülmüştür.

En iyi optimize edilmiş tek elemana dayalı olarak, 5G gereksinimlerini karşılamak için anten tasarımının yönlülüğünü ve gerçekleştirilen kazancını arttırmak için birkaç çift polarize mikroşerit anten dizisi tasarlanmıştır. Tek elemanlı ve düzlemsel dizileri tasarlamak için ticari simülasyon Studio Suite (CST) ve Advanced Design System (ADS) kullanılmaktadır.

6GHz altı 5G cep telefonlarında ve baz istasyonu sistemlerinde kullanılabilen iyi anten performansı sağlayan anten dizisini beslemek için paralel besleme teknikleri kullanılmıştır.

Anahtar Kelimeler: Çift kutuplu, Açıklık kuplaj, H-şekilli, Mikroşerit anten, Anten dizisi, Sub-6GHz, 5G haberleşmesi**.**

CONTENTS

NOMENCLATURE

λ	Wavelength
1G	First-Generation of Wireless Cellular Technology
2G	Second-Generation of Wireless Cellular Technology
3G	Third-Generation of Wireless Cellular Technology
3GPP	3rd Generation Partnership Project
4G	Fourth-Generation of Wireless Cellular Technology
5G	Fifth-Generation of Wireless Cellular Technology
BS	Base Station
BW	Bandwidth
FNBW	First Null Beam Width
HPBW	Half Power Beam Width
LTE	Long-Term Evolution
MIMO	Multi-Input Multi-Output
MS	Mobile Station
MSA	Microstrip Antenna
UMTS	Universal Mobile Telecommunication System
VSWR	Voltage Standing Wave Ratio
WWWW	Wireless World Wide Web

LIST OF TABLES

LIST OF FIGURES

CHAPTER 1

INTRODUCTION

The fifth-generation (5G) of wireless cellular technology is a term that mentions the next phase of mobile networks standard beyond 4G, whereas a new generation comes every ten years or so. 5G aims to enhance the network performance with high capacity and cheap cost, resulting in extremely high data rates for the customer. 5G communication systems will feature the technology of multi-input multi-output (MIMO), and the data rate will be 10Gbps [1].

5G frequency bands can be divided into two main ranges; the first range is the low band sub-6 (< 6GHz). Although previous generations have used some frequencies in this band, in 5G, it has extended to cover a potential new spectrum. The second range is the mm-wave band (> 24GHz). The networks in this band will operate on high frequencies known as millimeter waves and achieve high bandwidth over 1GHz. Millimeter wave frequencies require new techniques in designing the antennas for the mobile station (MS) and the base station (BS) systems [2].

To use high-frequency bands, 5G base stations must be placed a few hundred meters apart because high frequency signals cannot travel long distances. On the other hand, 5G signals which use low-frequency bands can use the base station of 4G and do not require more than base station upgrades [3].

High gain is necessary for 5G antennas, which can be possible by increasing the number of antennas and employing array configurations.

Table 1.1 gives a summary of mobile communications generations.

.

Table 1.1 A brief history of mobile communication generations [4].

Cellular generation	1G	2G	3G	4G	5G
First year deployment	1981	1992	2001	2010	2020
Frequency Bands	150MHz-900MHz	900MHz 1.8GHz	800-900MHz 1.6-2GHz	2GHz-8GHz	3GHz-300GHz
Peak data rate	2Kbps	64Kbps	2Mbps	100Mbps - 1Gbps	10Gbps
Technology	Analog	Digital	UMTS	LTE	WWWW

1.1 Literature Review

1.1.1 2x2 microstrip antenna array

- A dual polarization wideband microstrip antenna array has been presented in [5]. The antenna consists of four single elements arranged in a 2x2 layout. The antenna is resonant at 11.7GHz frequency, working in the Ku-band. In this paper, the S11 parameters show -10dB along the antenna bandwidth while the isolation between ports has reached better than -26 dB. The total gain of this antenna array has reached 11.73 and 11.72 in the two ports, respectively.

- A dual-band dual polarization microstrip antenna array has been presented in [6]. The operation frequencies are 30 GHz and 38 GHz. The single-element antenna has a suitable size, so the total size of the 2x2 antenna array was 0.8λ. The total gain of this antenna array has reached 9.89 dB and 8.43 dB in the two ports, respectively.

- A dual polarization aperture coupled microstrip antenna array has been presented in [7]. The antenna operates in the X-band. The antenna designed of many layers to increase the dual-polarized antenna array exhibits a bandwidth of 19.8% for vertical and 16.7% for horizontal ports. The isolation between ports has reached 33dB and 34dB in the two ports, respectively.

- Dual-band dual-polarized Microstrip Array for mm-Wave and sub-6 GHz Applications has been presented in [8]. An antenna was designed with an operation band of 5.48 GHz and 26.25 GHz with a maximum gain of 9.2dBi and 11.83 dB, respectively.

- Dual Polarization Microstrip Patch Array Antenna has been presented in [9]. In this paper, the antenna operates at 2.4 GHz with maximum gain of 9.5 dB.

1.1.2 4x4 microstrip antenna array

- A wideband aperture coupled microstrip antenna array has been presented in [10]. The antenna consists of four single elements arranged in a 4x4 layout. The antenna is resonant between 2.4 to 3GHz with a peak gain of 16.8 dB with a side lobe level of 15.3 dB. In this paper, the total size of the array is about 400x400x12.5 mm, which is a considerable size. The proposed antenna design in this thesis had a gain of 19.2dB with a smaller size.

- A 4x4 rectangular patch antenna array has been presented in [11]. The operation frequency is around 28 GHz. The proposed antenna has reached a bandwidth greater than 300MHz, and the total gain of the antenna array design is around 17 dB. The proposed antenna design in this thesis has a greater bandwidth with better gain.

- A 5x5 microstrip antenna array with L-probe feed technique has been presented in [7]. The design operates between 5.75-6.23 GHz. The array consists of 25 elements connected together using the series feed techquine. The antenna design has achieved a gain of 18.6 dB. The proposed antenna has reached better gain with a smaller number of elements.

- A 4x4 microstrip array for microwave radio communication system applications has been presented in[13]. The author has designed many antenna arrays to increase the antenna's gain. Yet, he has reached a maximum gain of 14.50 dB. The proposed antenna in this thesis has reached better gain with the same number of elements.

- A 4x4 L-probe Microstrip Patch Array Antenna has been presented in [14]. The antenna is presented for 60 GHz band applications. The antenna used a soft-surface to increase the gain and bandwidth of the antenna. The designed antenna has a complex structure, making it difficult to fabricate. However, the proposed design in this thesis is easy to fabricate.

1.2 Thesis motivation

The fifth-generation network system is expected to offer high data transfer speeds and reduced latency. For this purpose, academics and engineering teams throughout the globe are developing technologies that meet 5G specifications.

This thesis's primary objective is to serve sub-6GHz 5G base station systems by creating microstrip antennas that achieve all of the essential aspects of 5G base station requirements and specifications.

The proposed antenna has a broadband bandwidth, good impedance matching, good return loss level S11<-10 dB.

The proposed antenna design was optimized in a multi element array configuration to achieve the higher gain in order to be able to support the expected high data rates of the future 5G networks.

1.3 Thesis overview

The thesis is divided into five chapters.

Chapter one gives an introduction on the fifth generation of wireless cellular technology and an introduction of the microstrip antenna as well as research motivation and thesis arrangement.

Chapter two explains the background of antenna parameter. It specifies the fundamental antenna parameters, which include the radiation pattern, the beamwidth, and the directivity of the antenna. the realized gain, bandwidth, polarization, efficiency, and input impedance of the antenna also will be included. the categorization of antennas based on their physical structure will be described. Finally, the design

process for microstrip antennas will be shown.

Chapter three discusses aperture-coupled microstrip antennas, their characteristics, and the effects of the parameters on the antenna performance. Later in the same chapter, after considering all the factors affecting the antenna, single element aperture-coupled H-shaped microstrip antenna is conducted using CST Studio Suite ®. The optimized dual-polarized aperture-coupled microstrip antenna operating at 3300 – 3800 MHz frequency band and the simulations results is provided.

In Chapter four, antenna array design is presented; the array is constructed from the single element design of the dual-polarized H-shaped aperture-coupled microstrip antenna. The chapter consists of many array designs, including a 2x2 antenna array and a 4x4 antenna array.

Chapter five presents a summary of the research work, briefing on the most important findings and presenting the future work.

CHAPTER 2

ANTENNA THEORY

An antenna or Aerial can be defined as a metallic device for transmitting and receiving electromagnetic waves which convert electrical signals into electromagnetic waves and vice versa, Figure 2.1 shows the structure of the antenna. Also, the antenna is defined as the transition between guided electromagnetic waves and free space [15].

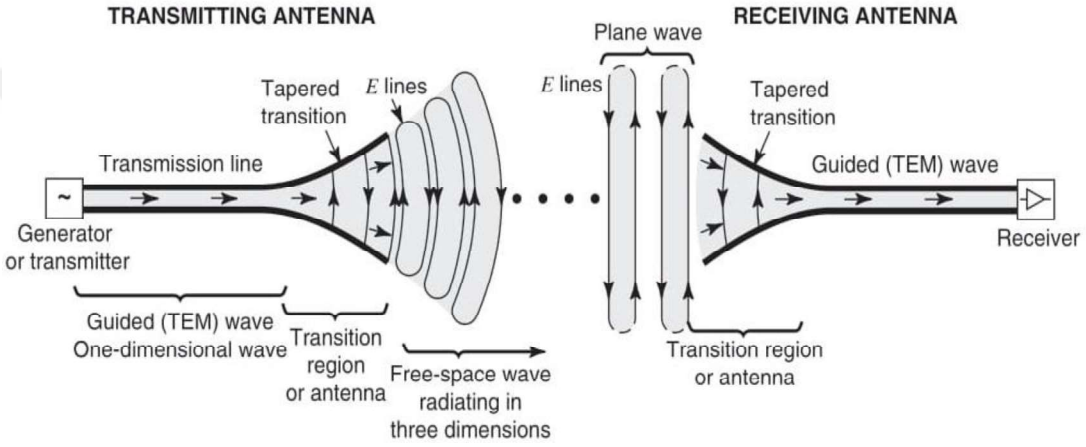

Figure 2.1 Transmitting and receiving antenna structure [16].

From Figure 2.1, we consider that antenna the antenna can function as both a transmitter and a receiver; thus, it is a reciprocal device. The antenna is crucial to the wireless system; without it, there is no wireless communication. The size and shape of antennas vary based on operating frequency and application.

Electrical circuits may be used to illustrate the antenna system. As shown in Figure 2.2, where an ideal generator source represents the source, the transmission line is represented by Z_c. A load represents, and the antenna Z_A [15].

$$Z_A = [(R_L + R_r) + jX_A] \quad \textbf{(2.1)}$$

Where R_L is referred to the conduction and dielectric losses, R_r is referred to the

radiation resistance, and X_A is referred to the imaginary part of the impedance. For this ideal case, the generator's energy must be converted into radiation resistance R_r [15].

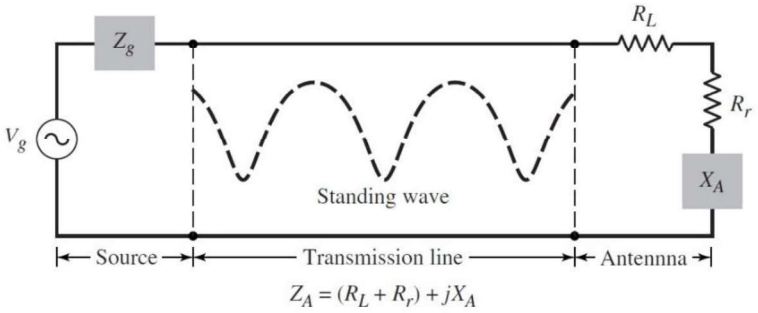

Figure 2.2 Thevenin equivalent of antenna in transmitting mode [15].

2.1 Antenna parameters

This section provides antenna design and measurement characteristics required to comprehend and describe antenna performance.

2.1.1 Radiation pattern

The antenna radiation pattern or antenna pattern is defined as a graphical representation of the antenna's radiation properties based upon the angular space. The field pattern represented the magnitude plot of the electric field and the magnetic field, while the power pattern represented the square plot of the electric field or the magnetic field.

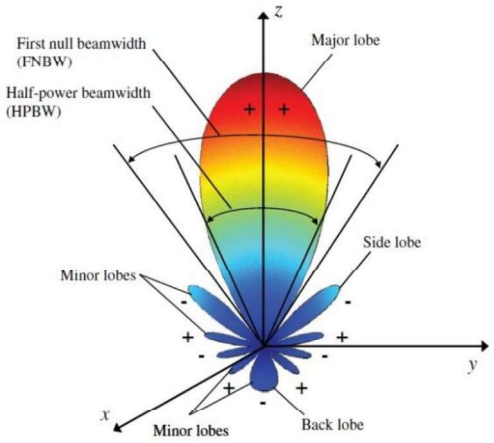

Figure 2.3 Radiation lobes and beamwidths of an antenna pattern [15].

Various sections of a radiation pattern are known as lobes, which may be subdivided into major, minor, side, and back lobes.

Three major shapes of radiation patterns describe an antenna's radiation property: isotropic, directional, and omnidirectional. The shapes are shown in Figure 2.3.

2.1.2 Beamwidth

Beamwidth of an antenna pattern is the angular distance between two identical places on the maximum opposing side of the pattern. There are several beamwidths in the antenna pattern, however the two most significant are the Half-power beamwidth (HPBW) and the first null beamwidth (FNBW). HPBW is defined as the angle between two identical spots when the intensity of radiation is half the beam's value. Meanwhile, FNBW is defined as the angular distance between the initial nulls of the antenna patterns [15]. Both HPBW and FNBW are shown in Figure 2.4.

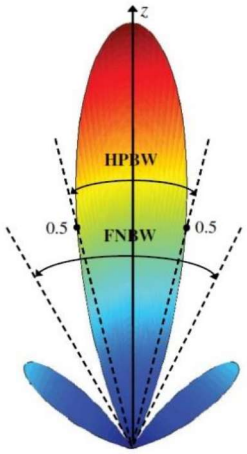

Figure 2.4 Two-dimensional power patterns [15].

2.1.3 Directivity

Directivity is a fundamental definition and antenna parameter. It is defined as the radiation intensity (U) ratio in a given direction from the antenna to the radiation intensity averaged over all directions. The average radiation intensity is equal to the total power radiated by the antenna divided by 4π. the following equation represents the mathematical form of the directivity.

$$D = \frac{U}{U_o} = \frac{4\pi U}{P_{rad}} \quad (2.2)$$

Where D referred to the directivity, U referred to the radiation intensity of the designed antenna, U_o is referred to the radiation intensity of the isotropic antenna, and P_{rad} is referred to the overall of the radiation power.

2.1.4 Antenna Efficiency

The efficiency of an antenna as measured by the ratio of radiated power to input power. There are several antenna efficiencies, for example, the total antenna efficiency e_o is used to take into account losses at the input terminals and within the structure of the antenna.

2.1.5 Antenna Gain

The antenna gain can be defined as the ratio between the intensity in a particular direction and the radiation intensity that would be achieved if the antenna absorbed power and radiated it isotropically. The definition of gain is so close to directivity. The only difference is that the gain takes into account the antenna's efficiency and its directional capabilities.

$$G = e_o D \quad (2.3)$$

2.1.6 Bandwidth

The antenna's bandwidth (BW) can be described as the frequency range between which the antenna's performance is optimal, concerning some characteristics, meets a specified standard. Where the antenna properties at the center frequency (such as radiation pattern, beamwidth, directivity, efficiency, gain, polarization, and input impedance) are within an acceptable range.

2.1.7 Polarization

Polarization is the characteristic of an electromagnetic wave that describes the time-

varying direction and amplitude of the electric-field vector.

Linear polarizations, circular polarizations, and elliptical polarizations are the three main types of polarization. Figure 2.5 shows these types of polarization.

Circular and linear polarizations are exceptional elliptical situations that result when the ellipse transforms into a straight line or a circle, respectively.

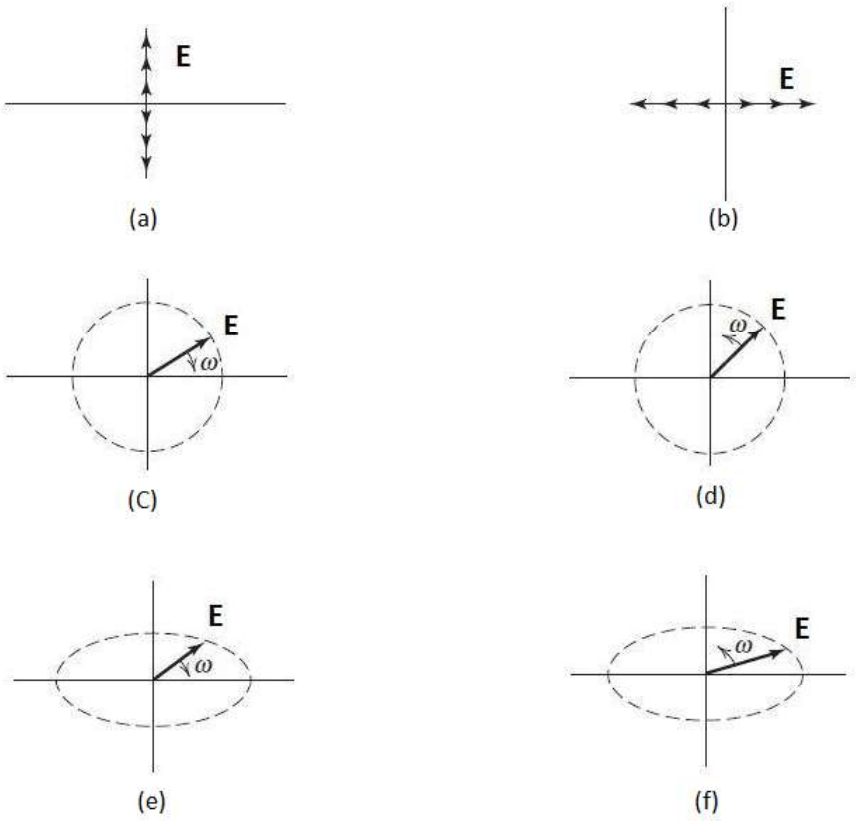

Figure 2.5 Types of polarization (a) vertical linear polarization, (b) horizontal linear polarization, (c) left-hand circular polarization, (d) right-hand circular polarization, (e) left-hand elliptical polarization, and (f) right-hand elliptical polarization [17].

2.1.8 Input impedance

The input impedance of an antenna is defined as voltage to current at a pair of terminals or the ratio of the appropriate components of the electric to magnetic fields at a point. The antenna can be represented as an equivalent electrical circuit. The antenna impedance is composed of real and imaginary parts as

$$Z_A = R_A + jX_A \quad \textbf{(2.4)}$$

Where Z_A is referred to as the antenna impedance, R_A is referred to as the antenna resistance, and X_A is referred to as the antenna reactance.

2.2 Types of antennas

There are many types of antennas. We will mention the most important ones.

2.2.1 Wire Antennas

Wire antenna is the oldest type of antenna. The wire antennas are composed of solid wire and are less expensive and simpler to manufacture than other forms. There are many shapes of wire antennas, such as straight wire (dipole), loop wire, and helix wire. These types are shown in Figure 2.6.

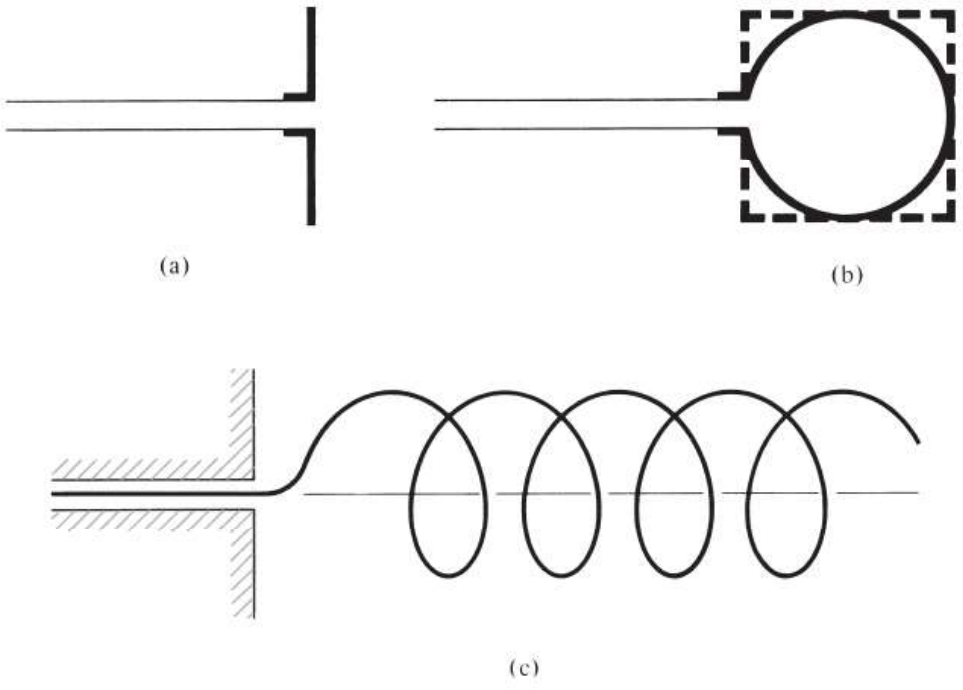

Figure 2.6 Wire antenna (a) dipole, (b) circular loop, and (c) helix [15].

2.2.2 Aperture Antennas

Aperture antennas are used in higher frequencies. It is used in many applications like aircraft and spacecraft. The famous form of aperture antennas are the pyramidal horn, conical horn, and the rectangular waveguide, which are shown in Figure 2.7.

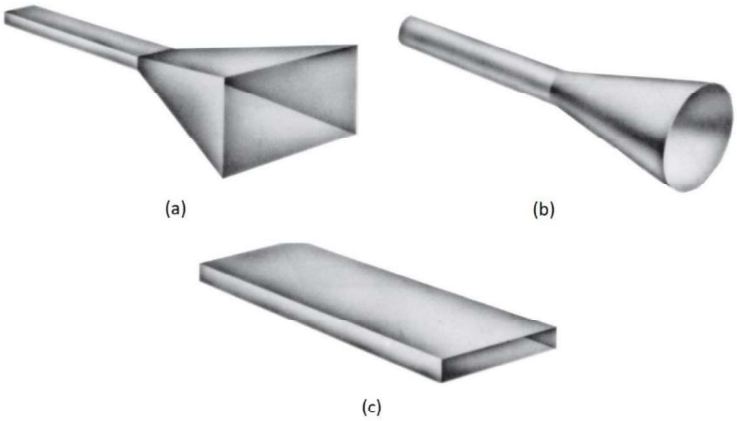

Figure 2.7 Aperture antenna (a) pyramidal horn, (b) conical horn, and (c) rectangular waveguide [15].

2.2.3 Reflector Antennas

The idea of reflector antennas is that they can be used to communicate over great distances. It used to broadcast and receive signals that required millions of kilometers of travel. During World War II, the reflector antenna was initially employed for radar applications and space communication. Today, our homes employ satellites to receive television broadcasts. Figure 2.8 shows the famous types of reflector antennas.

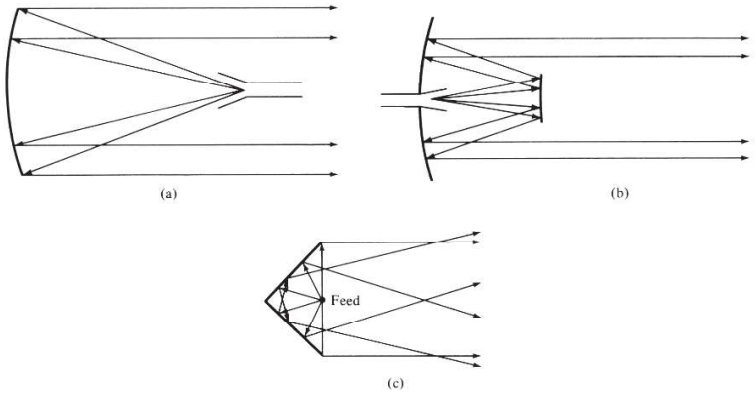

Figure 2.8 Reflector antenna (a) parabolic reflector with front feed, (b) parabolic reflector with Cassegrain feed, and (c) corner reflector [15].

2.2.4 Lens Antennas

Lens antennas focus the wave on the specified direction and prevent it from spreading in undesired directions. Lens antennas are categorized by their construction material or by their geometrical form.

2.3 Microstrip antenna

In recent years, there has been a need for low-profile antennas to be employed in a wide range of modern microwave systems. Microstrip antennas (MSA) have been found to meet these requirements. Figure 2.9 shows the structure of the microstrip antenna.

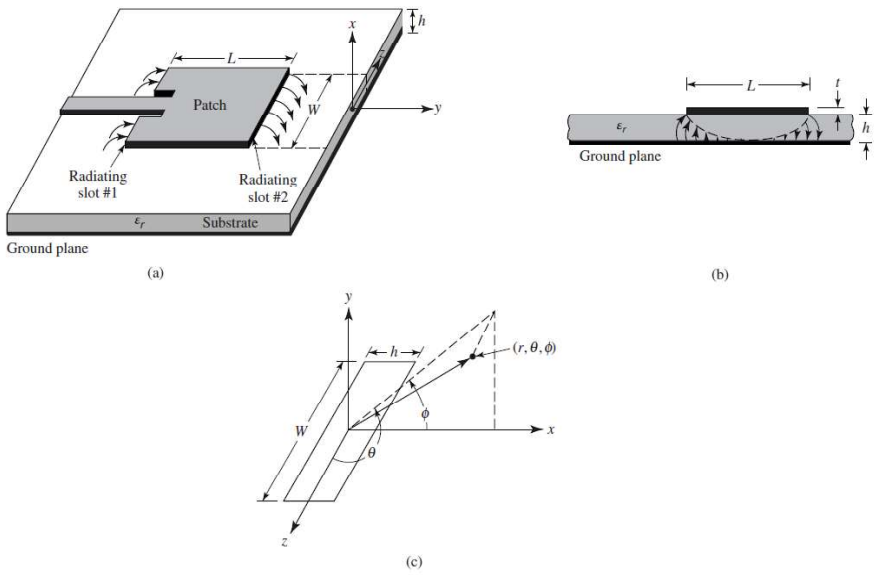

Figure 2.9 Microstrip antenna and coordinate system (a) Microstrip antenna, (b) Side view, and (c) Coordinate system [15].

The microstrip antenna is made up of a metal patch, a dielectric substrate, and a ground plane. The patch is on one side of the dielectric substrate, and the ground plane is on the other. There are several patch forms for microstrip antennas. The rectangular patch antenna is the most often used type due to its favourable radiation properties and ease of production. Figure 2.10 shows different shapes of the radiation part of microstrip antennas [15].

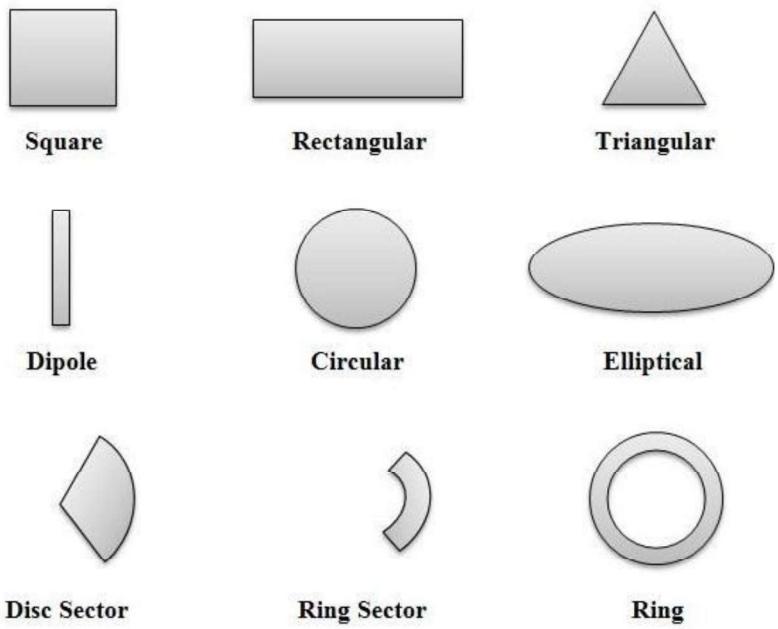

Figure 2.10 Shapes of microstrip patch elements [15].

The microstrip antenna design dates back to the 1950s [18]. However, the first practical implementations were performed in the early 1970s [19]. Since then, due to its multiple benefits, microstrip antennas have been extensively used in several communication systems.

The main advantage of the microstrip antenna is that it is small and cheap, which makes it ideal for systems like mobile communication infrastructures.

Microstrip antennas are manufactured using a limited number of materials. Therefore, Microstrip antennas are small and inexpensive to manufacture. Additionally, because microstrip antennas have a low profile, a tiny volume, and adhere to any surface due to the thin and flexible dielectric material. The microstrip antennas have adjustable radiation mechanisms, which means that the microstrip antenna polarization can easily change. Also, it is simple to make dual polarization and dual frequency operations. More than the advantages in fabrication, the microstrip antenna is used to design smart antennas when combined with phase shifter or PIN-diode switches. It is vital to describe the drawbacks of microstrip antennas in order to promote awareness of the precautions that should be taken while designing the antenna.

First, the microstrip antenna has a poor gain compared to other kinds of antennas. Also, the efficiency levels are poor. The following significant drawback of the microstrip antenna is the limited bandwidth. The gain of the microstrip antenna can improve by creating an array of multiple patch components, while a second resonant structure or an appropriate feeding mechanism can increase a microstrip antenna's bandwidth.

There are four most popular methods to feed the microstrip antenna. These four feeding strategies may be split into two broad categories: contacting and non-contacting. The contacting method means direct contact between the feed line and the radiating patch. The popular type of this method is microstrip line and coaxial probe. On the other hand, in the non-contacting method, the feeding is formed with no direct connection between the feeding line and the radiating patch. The popular types of this method are aperture coupling and proximity coupling. Figure 2.11 shows the typical feeds of the microstrip antennas [15].

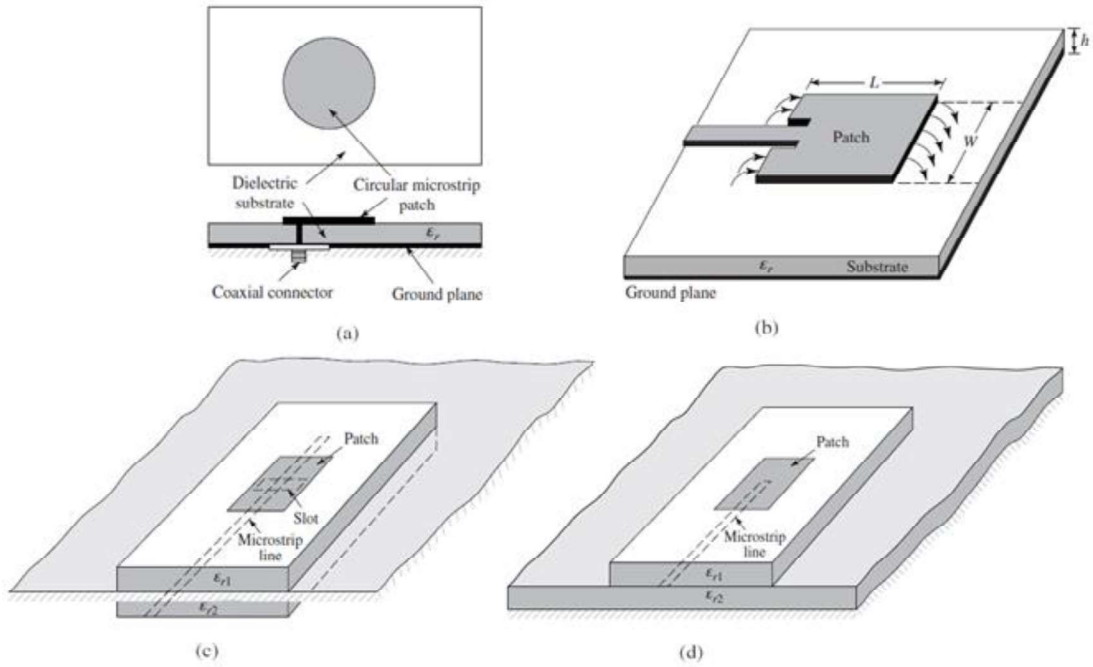

Figure 2.11 Typical feeds of the microstrip antennas, (a) probe feed, (b) microstrip line feed, (c) aperture-coupled feed (d) proximity-coupled feed [15].

Most applications use the first two feeding techniques (a) and (b) owing to their ease of fabrication and the availability of analytical methodologies or equivalent circuit models that facilitate antenna analysis. The primary disadvantage of these feed systems is the restricted of the dielectric substrate and the narrow bandwidth.

Due to the rise in fringing fields between the patch edge and the ground plane, Bandwidth is increased when a microstrip antenna is printed on a thick dielectric substrate with a low dielectric constant [20]. Thus, a thick substrate in a coaxial probe feed configuration corresponds to a lengthy inner conductor, which results in the antenna having an inductive input impedance. This leads to having a problem in matching the antenna. Included capacitive elements in the feed can solve this problem. However, this will make the manufacturing process becoming complicated.

The thick dielectric substrate with a low dielectric constant generates spurious feed radiation, degrading the antenna's performance [15]. Using dielectric substrates with varied dielectric constants for the radiating and feeding components of the device, such as in proximity coupled and aperture coupled feed systems, may solve this problem.

In mobile communication systems, dual-polarized antennas boost the received signal, limit the effects of multipath fading, and enhance the channel by doubling the transmission capacity per frequency [21].

Dual-polarization functioning is achieved in a microstrip antenna by concurrently excitation of the two orthogonal modes of the radiating patch. Hence, aperture coupled feed structure offers isolation between the two feed lines better and more effectively than the proximity coupled feed, which reduces the cross-polarization between the two feeds. Compared to proximity coupled feed, aperture coupled feed also offers many optimization parameters such as the aperture shape, the aperture dimensions, and the aperture position. As a result, this thesis examines aperture coupled feed structures.

CHAPTER 3

SINGLE ELEMENT DUAL-POLARIZED APERTURE-COUPLED ANTENNA

3.1 Introduction

Aperture-coupled microstrip antennas consist of two dielectric substrates separated by a ground plane. The microstrip patch is printed on the top surface of the upper substrate. In contrast, the microstrip feed line is printed on the bottom of the lower substrate. The coupling aperture is located on the ground plane between the top and the bottom substrates, and the microstrip feed line is coupled to the patch through the slot. Figure 3.1 shows the geometry of the basic aperture coupled microstrip antenna [22].

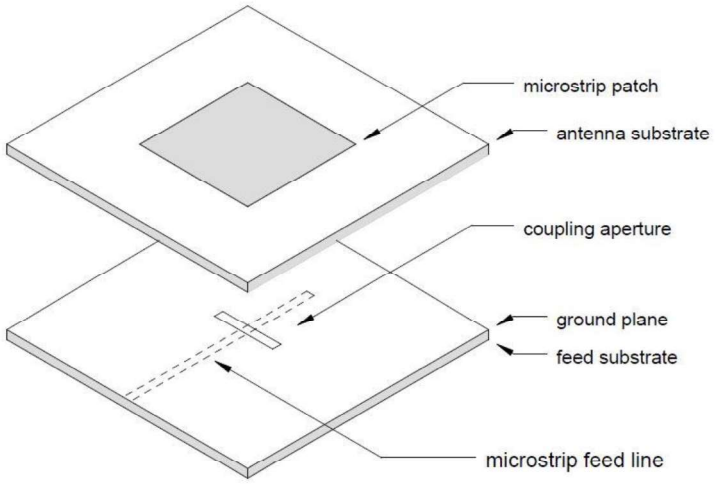

Figure 3.1 Geometry of the basic aperture coupled microstrip antenna [22].

The first aperture coupled microstrip antenna was fabricated and tested by a graduate student, Allen Buck, in 1984 [23]. However, the original prototype antenna used circular coupling aperture. Researchers today use different slot shapes to optimize antenna radiation and coupling characteristics. Figure 3.2 shows different shapes of the coupling slot [24].

It is required to use an aperture design that maximizes coupling while using the least amount of area. Slot with enlarged ends, like bowtie, Hourglass, and H-shaped, meets these requirements. These slots improve the coupling of the antenna and result in a significant impedance bandwidth. In addition, it decreases the level of antenna back radiation.

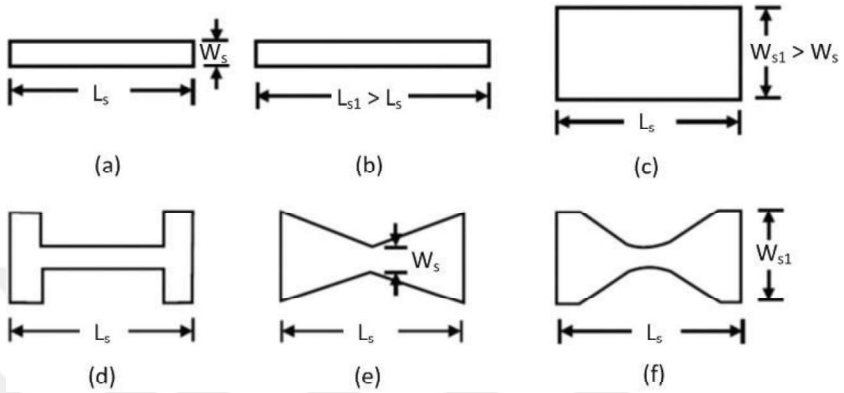

Figure 3.2 Different shapes of coupling slot: (a) thin rectangular, (b) longer rectangular, (c) wider rectangular, (d) H-Shaped, (e) bowtie-shaped, and (f) hourglass-shaped [24].

3.2 Transmission-Line Analysis of the Aperture-Coupled Patch Antenna

There are several methods for analyzing microstrip antennas. The transmission line model, cavity model, and method of segmentation are simple and useful methods that give physical insight into the antenna's radiation process. However, these approximation methods and their accuracy are inferior when comparison with the Integral Equation method, which is based on the numerical solution of integral and differential equations associated with the structure. Still, this method requires a large amount of computational time.

The aperture-coupled microstrip antenna is analyzed using a transmission-line approach to have a quick and efficient method for computing the radiating patch's parameters and the antenna's other parameters. The geometry of an aperture-coupled microstrip antenna is shown in Figure 3.3.

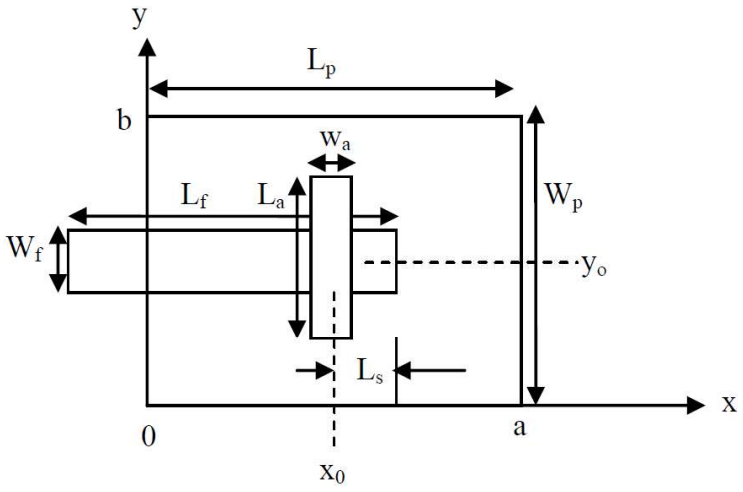

Figure 3.3 Geometry layout of Aperture-coupled Patch Antenna [25].

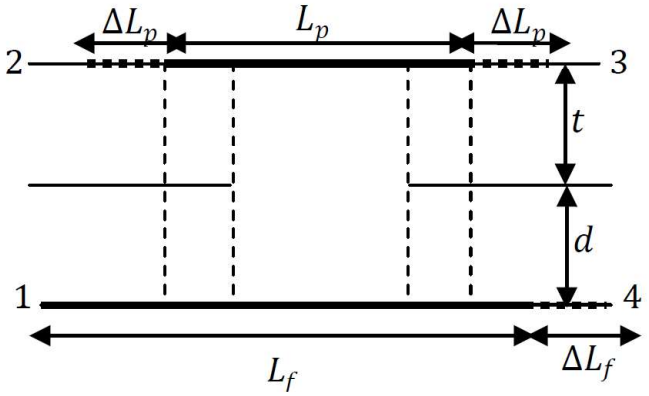

Figure 3.4 Aperture coupled microstrip antenna system for analysis (Side view) [25].

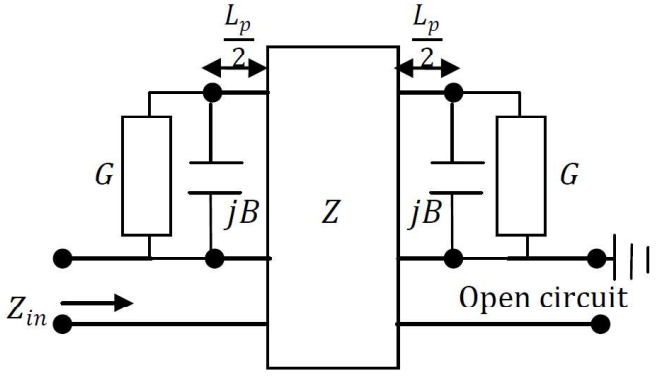

Figure 3.5 Transmission line model of the aperture coupled microstrip antenna [25].

The resonant frequency of the rectangular patch antenna, which is the wavelength

divided by two in its fundamental mode, is determined by the resonant length. In its fundamental mode, the length and width are calculated by the formulas [26]:

$$L_p = 0.49\frac{\lambda_0}{\sqrt{\varepsilon_r}} \quad (3.1)$$

$$W_p = \frac{c}{2f_0}\sqrt{\frac{2}{\varepsilon_r + 1}} \quad (3.2)$$

As shown in Figure 3.4 due to the fact that the dimensions of the patch are not infinite, which causes fringe fields on the edges, the Physical dimensions of the microstrip antenna seem greater than its actual dimensions. "The fringing fields at the two open ends are accounted for by adding equivalent lengths ΔL_p and ΔL_f at both ends. The expression for ΔL_p and ΔL_f are given as" [27].

$$\Delta L_p = 0.412t\frac{(\varepsilon_p + 0.3)(\frac{W_p}{t} + 0.263)}{(\varepsilon_p + 0.258)(\frac{W_p}{t} + 0.813)} \quad (3.3)$$

$$\Delta L_f = 0.412d\frac{(\varepsilon_f + 0.3)(\frac{W_f}{d} + 0.263)}{(\varepsilon_f + 0.258)(\frac{W_f}{d} + 0.813)} \quad (3.4)$$

Where ε_p and ε_f are the effective dielectric constants of the patch substrate and the feedline substrate, and t and d are the thickness of the patch and feedline, respectively.

The effective lengths of the patch and feedline are given as

$$L'_p = L_p + 2\Delta L_p \quad (3.5)$$

$$L'_f = L_f + \Delta L_f \quad (3.6)$$

Figure 3.5 show the radiation conductance at these ends because the patch radiates electromagnetic energy mostly through the two narrow slots at the two open ends of the patch. G is utilized to indicate the radiation conductance is given as

$$G = \frac{\sqrt{\varepsilon_{eff}}}{240\pi^2} F(\sqrt{\varepsilon_{eff}} \frac{2\pi}{\lambda_0} w_e) \quad (3.7)$$

$$\varepsilon_{eff} = \frac{\varepsilon_r + 1}{2} + \frac{\varepsilon_r - 1}{2} [1 + \frac{12h}{w}]^{-1/2} \quad (3.8)$$

$$w_e = \frac{120\pi h}{z_o \sqrt{\varepsilon_{eff}}} \quad (3.9)$$

Where is w_e the effective width which is takes into account the fringing effects and ε_{eff} and z_o are the effective dielectric constant and the characteristic impedance respectively.

3.3 Parameters of Aperture Coupled Microstrip Antennas

During the design process for aperture-coupled microstrip antennas, several parameters must be examined and investigated. These parameters and their effects are summarized below:

- Antenna Substrate Dielectric Constant

This parameter affects the efficiency and the bandwidth of the antenna. Microstrip antenna with high dielectric constant substrate suffers from narrow bandwidth and low efficiency so; It is preferred to choose a substrate with a low dielectric constant to maximize the bandwidth and radiation efficiency of the antenna.

- antenna substrate thickness

This parameter affects the coupling level and the bandwidth of the antenna. While increasing the thickness of the antenna substrate, the bandwidth will increase, However, the amount of coupling between the aperture and the microstrip patch will decrease. These implications should be considered while modifying this value.

- Microstrip Patch Width and Length

The width and length of the patch determine the antenna's resonant frequency. Wider

patch will lead to a decrease in resonant resistance. When the patch's length and width are selected to be equal, the cross-polarization level will increase. On the other hand, In the case of dual-polarization and circular polarization, a square patch arrangement is recommended.

- Feed Substrate Dielectric Constant

Microstrip feed line should have higher dielectric constant substrate. While higher dielectric constant results in losses in the antenna. So, the dielectric constant of the substrate Feed must range between 2 and 10.

- Feed Substrate Thickness

This value has an effect on the spurious radiation emitted by the feed line. For less unnecessary radiation, Feed substrate thickness must fall between 0.01λ and 0.02λ.

- Feed Line Width and Length

Width and length of the feed line determine the characteristic impedance and coupling level between aperture and feed line. The thinner feed line couple more strongly to the aperture.

- Length of Tuning Stub

This parameter is used to adjust the slot-coupled antenna's excess reactance. Typically, the stub is shorter than $\lambda g/4$ in length. The impact of the stub length is to rotate the whole impedance locus on the Smith chart either upwards or downwards.

- Slot Width and Length

The slot's width and length are critical parameters that affect the resonance frequency, coupling level between the microstrip patch and the microstrip feed line, and back radiation level. Therefore, the slot should be made no larger than is required for impedance matching. The ratio of slot length to width is typically 1/10.

- Position of the Slot

The position of the slot affects the coupling between microstrip patch and microstrip feed line. For maximum coupling level, the patch should be centered over the slot, and the feed line should be positioned at the right angles to the center of the slot.

3.4 Single element Aperture-Coupled Microstrip Antenna

Design, and simulation results for a dual-polarized H-shaped aperture coupled microstrip antenna will are presented; All the analyses are done at the N78 operation band according to 3GPP specifications which it is 3300 – 3800 MHz and the center frequency of the design is adjusted at 3.5 GHz.

H-shaped slots on the ground plane are used to couple the patch to the feed line; they offer a broadband characteristic with a shorter slot length than other shapes such as rectangular, bowtie, and hourglass slots [25]. two orthogonal H-shaped slots are presented in order to apply the dual-polarized characteristic. At this configuration, the mutual coupling between these two slots is investigated.

The antenna is designed using two dielectric substrates. The microstrip patch is located below the first dielectric substrate, while the microstrip feed line is below the second dielectric substrate. The ground plane is installed between the two dielectric substrates. Figure 3.6 and Figure 3.7 show the dielectric constant values and the antenna's structure.

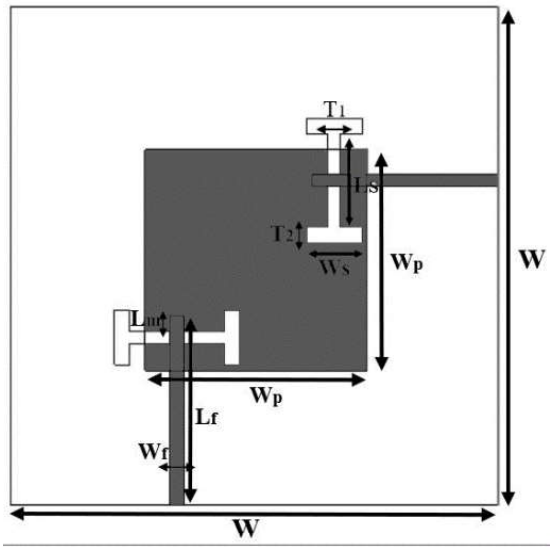

Figure 3.6 Dual-polarized H-shaped aperture coupled microstrip antenna structure (top view).

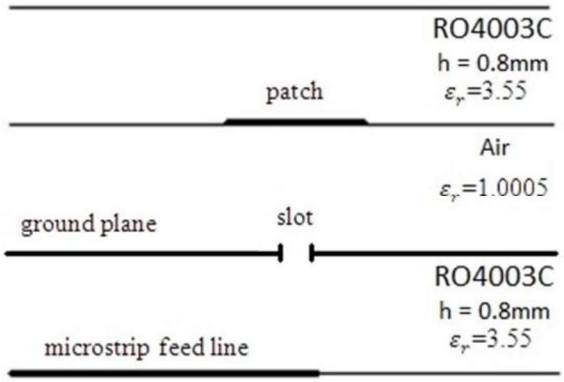

Figure 3.7 Dual-polarized H-shaped aperture coupled microstrip antenna structure (side view).

By supplying the patch with two H-shaped slots, dual polarization might have been accomplished, the slots have been positioned in a T-shape for optimal isolation, as shown in Figure 3.6. The antenna has been designed using CST microwave studio Suite and the parameters of the antenna are optimized and listed in Table 3.1.

Table 3.1 Optimized parameters of dual-polarized aperture coupled microstrip antenna with H-shaped slot.

Design Parameter	Description	Value (mm)
W	Microstrip antenna length and Width	61.92
Wp	Antenna patch length and width	28.10
Ws	H-shaped slot width	11.80
Ls	H-shaped slot length	7.05
T1	H-shaped slot center leg thickness	1.56
T2	H-shaped slot side leg thickness	1.97
Wf	Microstrip feed line width	1.68
Lf	Microstrip feed line width	21.14
Lm	Stub length	2.81
Off	X and y direction offset	10.00
T	Antenna patch thickness	0.035
D1	upper substrate thickness	0.80
D2	lower substrate thickness	0.80
D3	Air thickness	6.55

The parametrical analyses of the designed aperture coupled microstrip antenna are given in subsections below.

3.4.1 The Parametrical Analysis of the Stub Length

This section gives the effects of the length of the stub on resonant frequency and bandwidth characteristics. The analysis of the stub length change is done between 2mm and 8mm. Return loss and isolation between ports are investigated in Figure 3.8 and Figure 3.9.

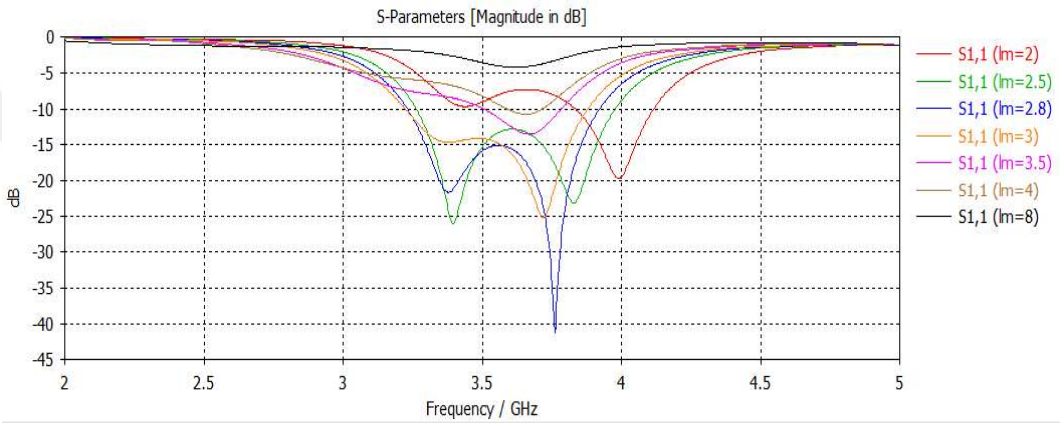

Figure 3.8 The return loss S11 as a function of the stub length of the microstrip antenna.

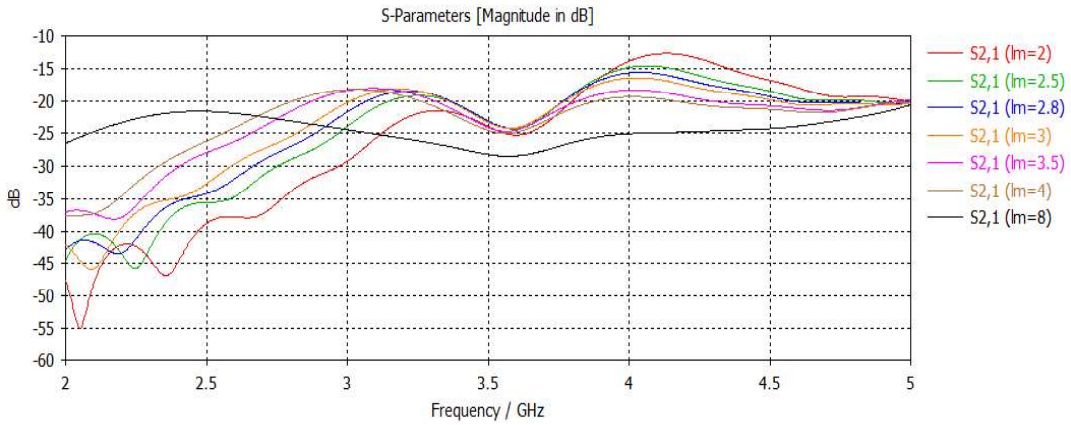

Figure 3.9 The isolation between port S21 as a function of the stub length of the microstrip antenna.

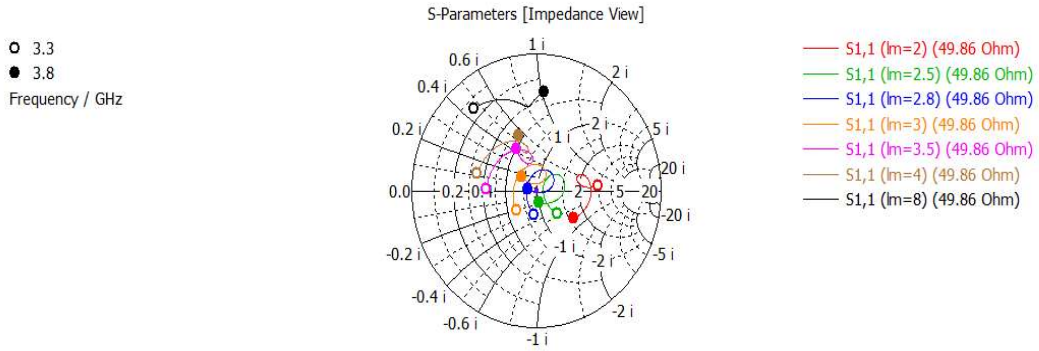

Figure 3.10 Smith chart of the stub length analysis of the microstrip antenna.

Figure 3.10 shows the smith chart of the analysis of stub length. It clearly when the length of the stub increases, the input impedance curve moves in inductive direction.

3.4.2 The Parametrical Analysis of the length of H-shaped slot

This section gives the effects of the length of H-shaped slot on the resonant frequency and isolation between ports of the antenna. The analysis of the length of H-shaped slot change is done between 6mm and 14mm. Return loss and isolation between ports are investigated in Figure 3.11 and Figure 3.12.

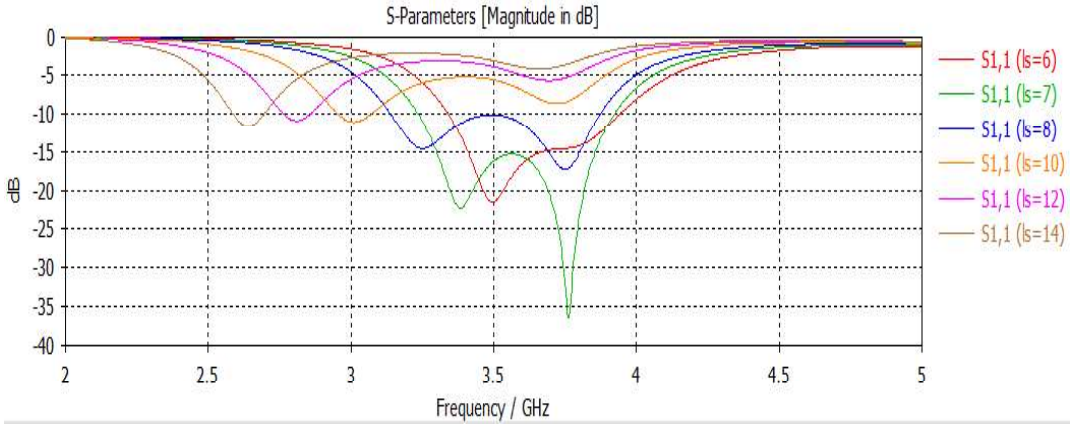

Figure 3.11 The return loss S11 as a function of the length of H-shaped slot.

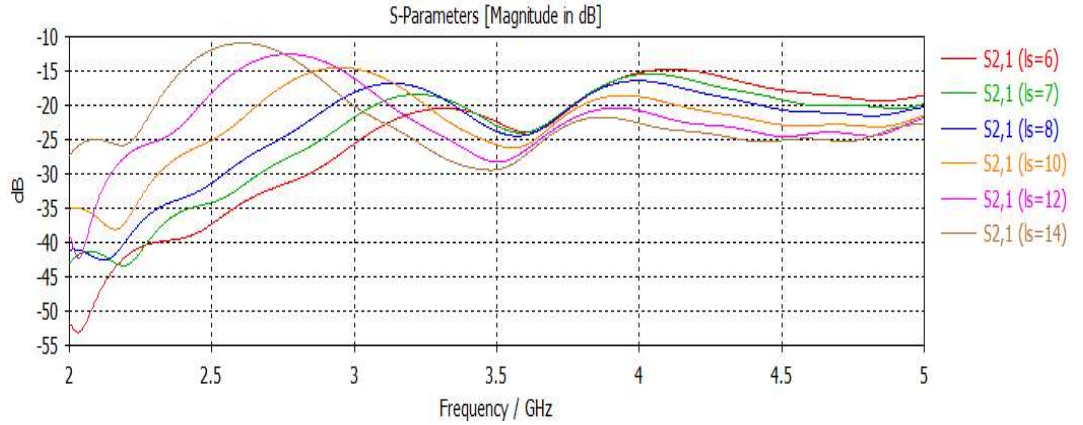

Figure 3.12 The isolation S21 as a function of the length of H-shaped slot.

Figure 3.11 shows that the coupling level changes when the center arm's length changes. When the center arm's length increases, the resonant frequency of the antenna changes, and the bandwidth decreases.

3.4.3 The Parametrical Analysis of the width of H-shaped slot

This section gives the effects of the width of H-shaped slot on the resonant frequency and isolation between ports of the antenna. The analysis of the width of H-shaped slot change is done between 6mm and 20mm. Return loss and isolation between ports are investigated in Figure 3.13 and Figure 3.14.

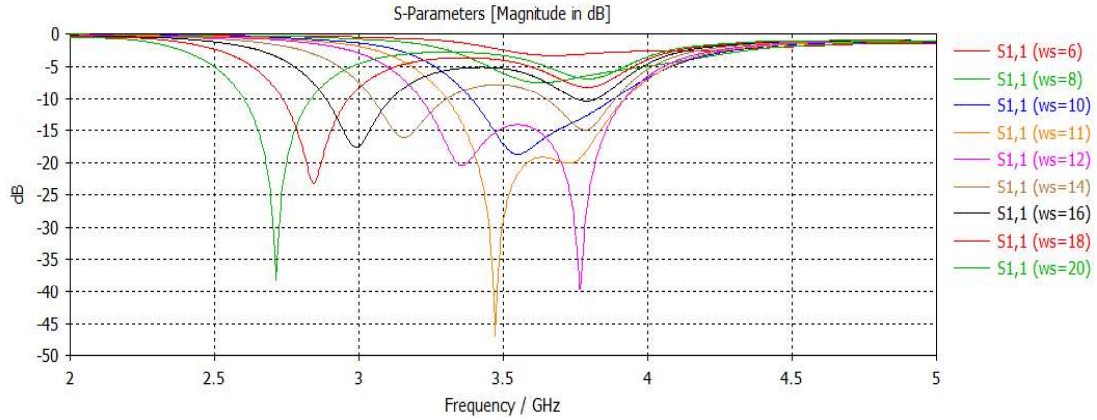

Figure 3.13 The return loss S11 as a function of the width of H-shaped slot.

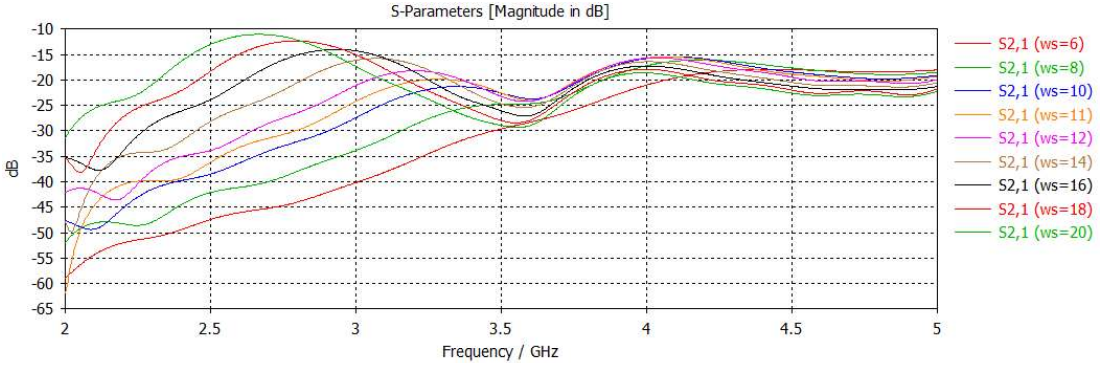

Figure 3.14 The isolation S21 as a function of the width of H-shaped slot.

Figure 3.13 shows that the effect of the width of the side arm of the H-shaped slot on the resonance frequency and bandwidth is the same as the length of the center arm. Hence, using an H-shaped provides additional parameters to optimize the resonance frequency and bandwidth of the antenna.

3.4.4 The parametrical analysis of the feedline position

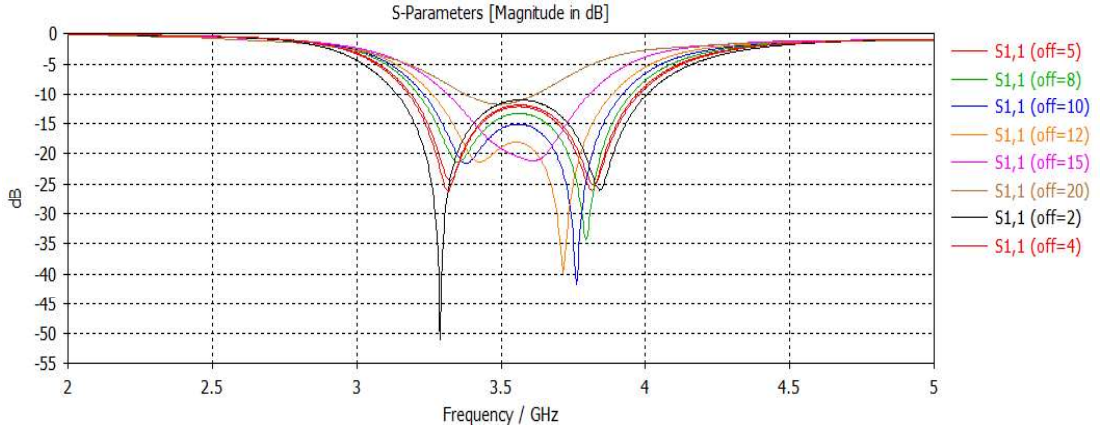

Figure 3.15 The return loss S11 as a function of the feedline position.

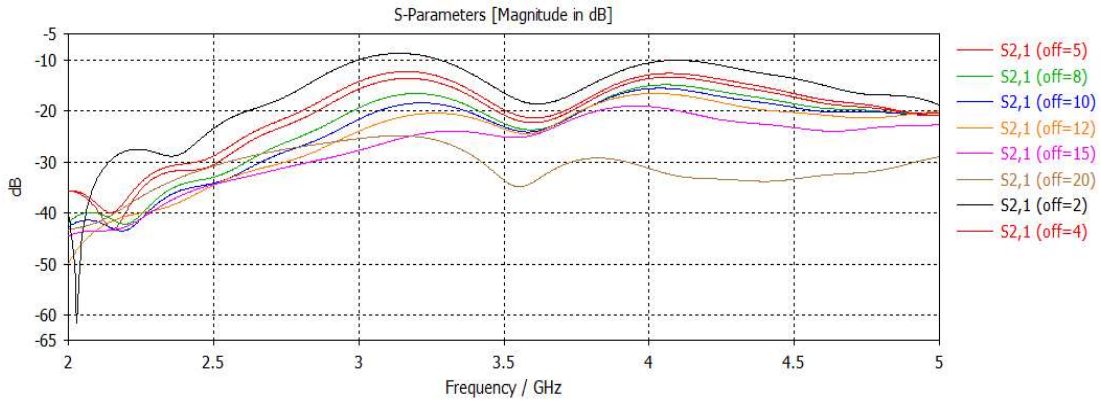

Figure 3.16 The isolation S21 as a function of the feedline position.

Figure 3.15 shows the effect of the feedline on the resonance frequency and bandwidth. Figure 3.16 shows the effect of feedline position on the isolation between ports as the isolation S21 becomes smaller when the two ports close each other.

3.4.5 The parametrical analysis of the air height

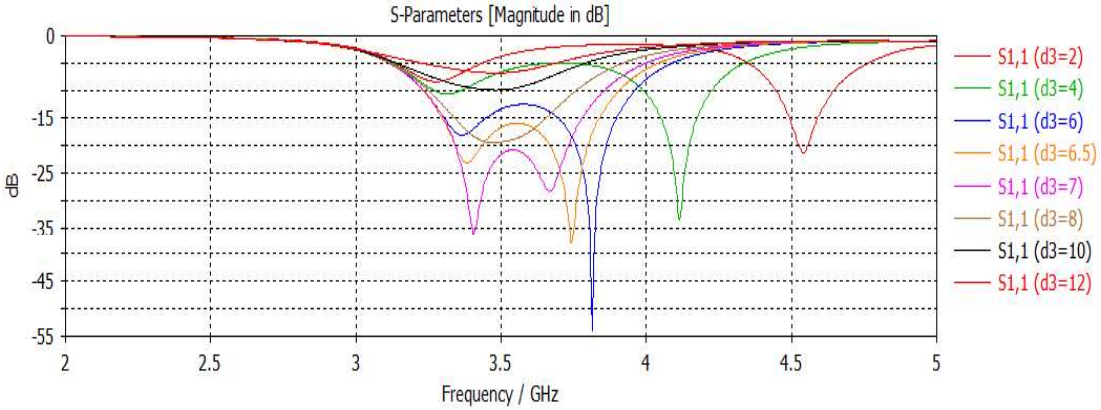

Figure 3.17 The return loss S11 as a function of the air height.

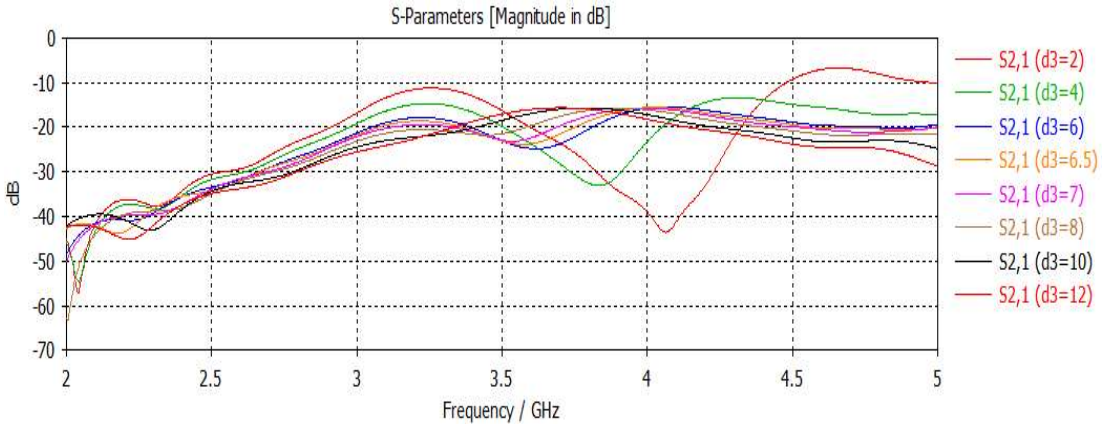

Figure 3.18 The isolation S21 as a function of the air height.

This section gives the effects of the height of the air on the resonant frequency and isolation between ports of the antenna. The analysis of the height of the air change is done between 2mm and 12mm. Return loss and isolation between ports are investigated in Figure 3.17 and Figure 3.18.

The simulation results for the dual-polarized single element are presented, the magnitude of the S11, S22 parameters has a good result larger than -15 dB in the region of 3.2 GHz to 3.92 GHz with a bandwidth of 0.5 GHz, as shown in Figure 3.19.

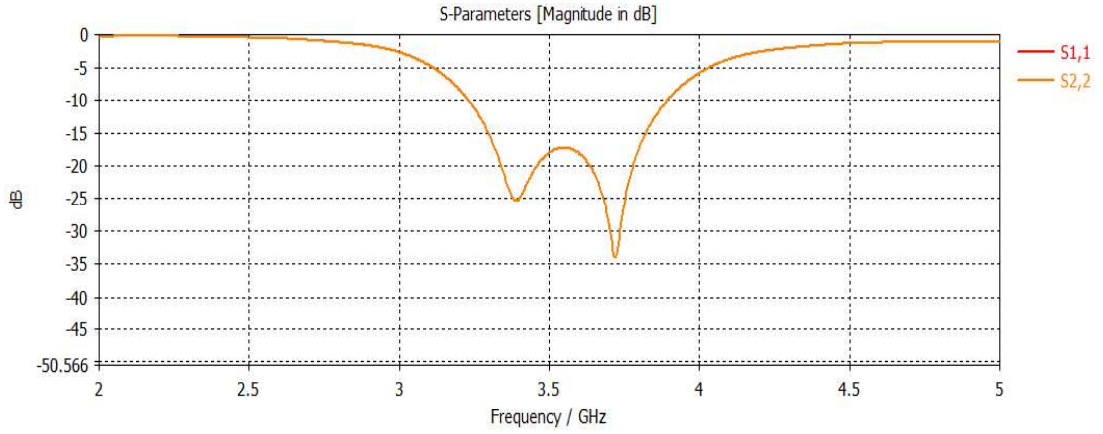

Figure 3.19 Simulation result of the return loss S11 and S22 for the single element.

Figure 3.20 shows that the isolation between the two ports, S21 and S12, has reached larger than -19 dB, while Figure 3.21 shows the value of voltage standing wave ratio (VSWR) for the two ports which is better than 1.42.

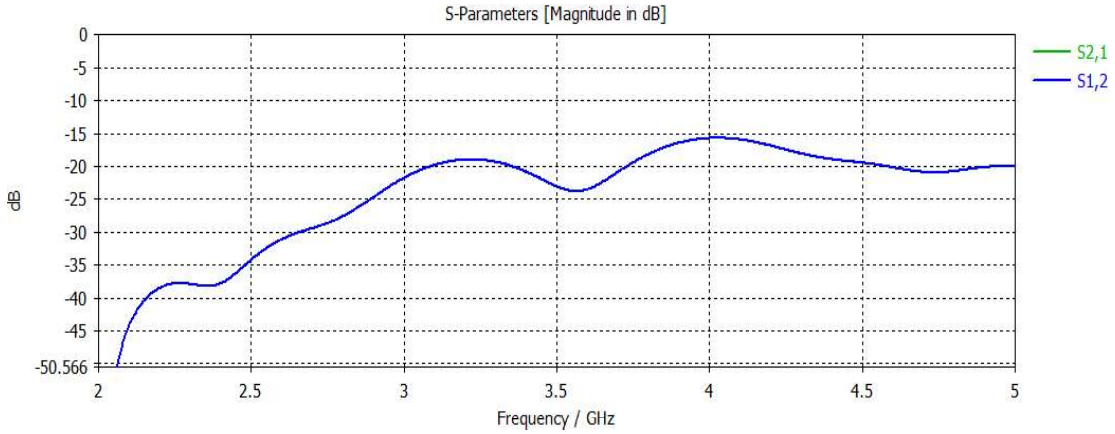

Figure 3.20 Simulation result of the isolation between ports S21 and S12 for the single element.

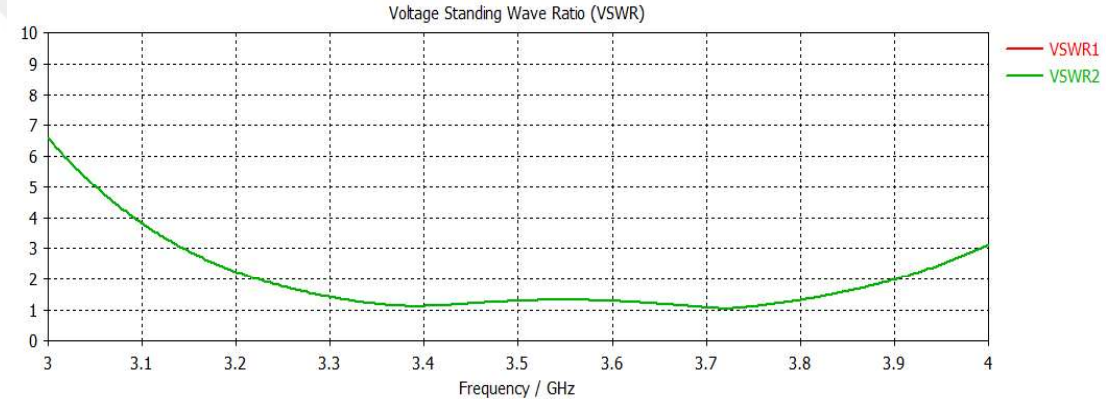

Figure 3.21 Voltage standing wave ratio (VSWR) simulation result

The radiation pattern of the dual-polarized H-shaped aperture-coupled microstrip antenna was measured at 3.5 GHz. Figure 3.22, and Figure 3.23 show the normalized E-plane radiation patterns of the two ports for co-polarization and cross-polarization components of the radiation pattern.

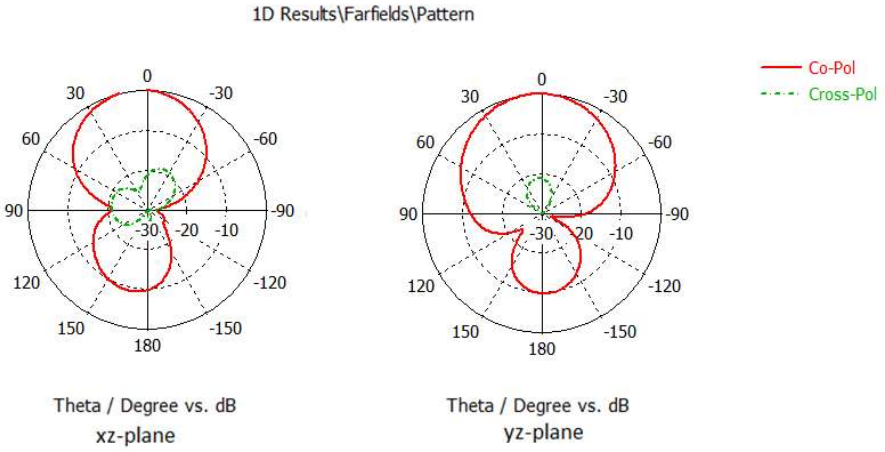

Figure 3.22 Radiation pattern of the single element for port1.

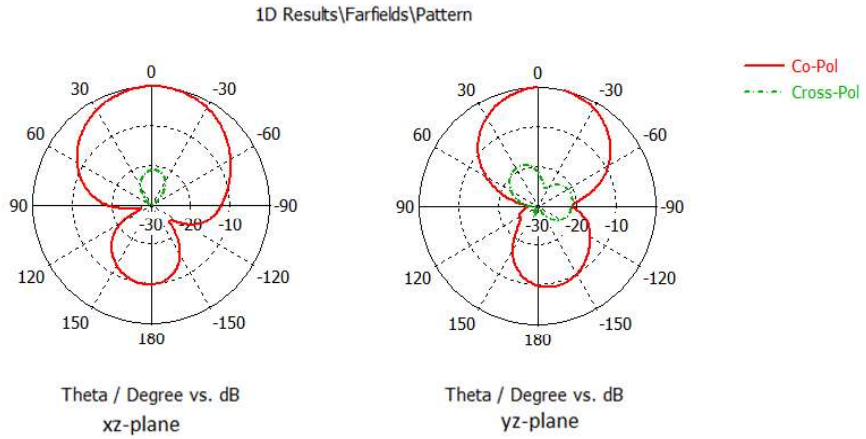

Figure 3.23 Radiation pattern of the single element for port2.

From the simulated radiation pattern, a good level of cross-polarization is determined between the two ports which is better than 19 dB.

The maximum realized gain for the dual-polarized H-shaped aperture coupled microstrip antenna is 8.27 dB for both of port 1, and Port 2. Figure 3.24 shows the three-dimensional radiation pattern for both port 1, and port 2. Figure 3.25 shows the realized gain of the antenna compare with frequency.

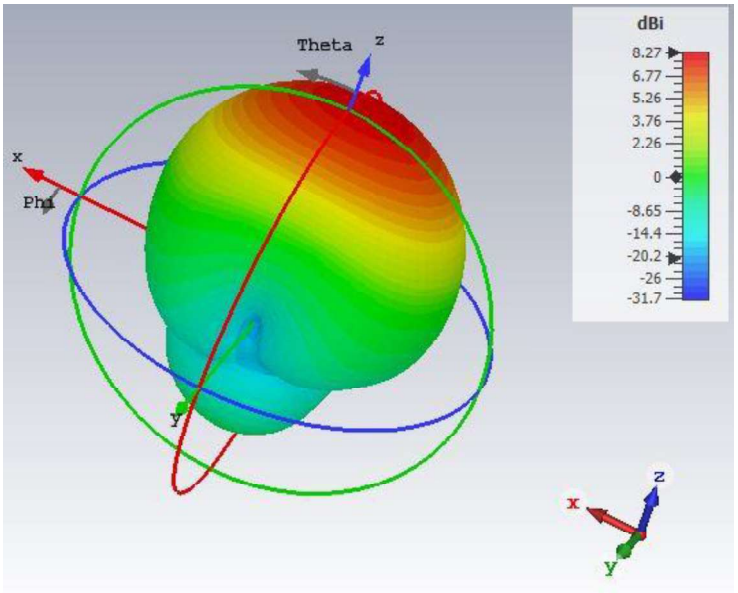

(a)

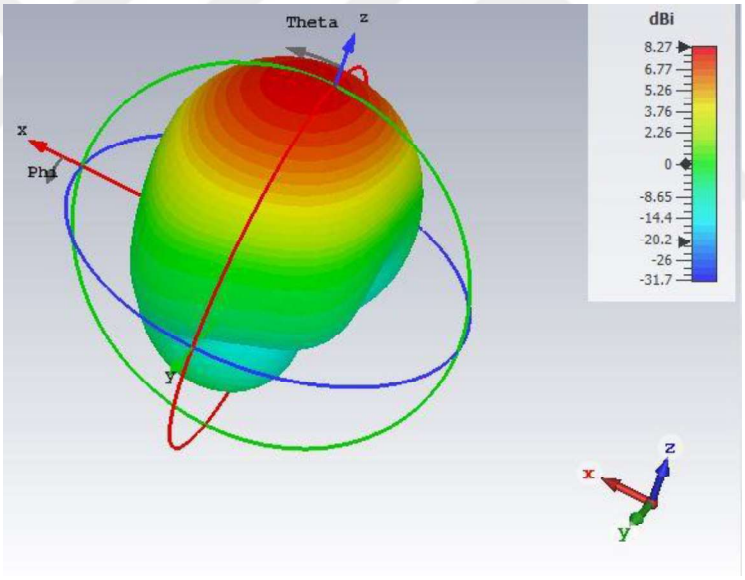

(b)

Figure 3.24 Three-dimensional radiation pattern (a) Port 1, and (b) Port 2.

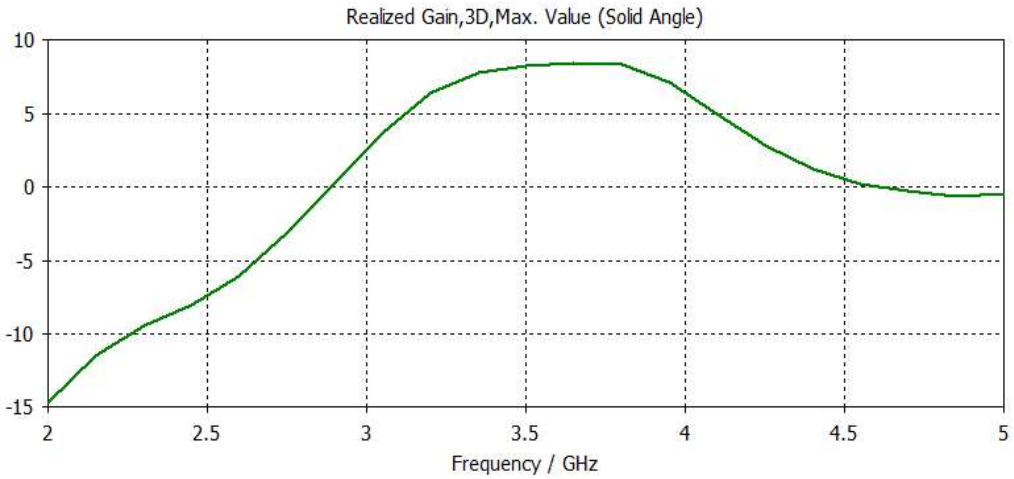

Figure 3.25 The realized gain of the single element microstrip antenna.

CHAPTER 4

ANTENNA ARRAY

Gain is a fundamental antenna characteristic when the antenna is intended to transmit and receive signals in a predetermined direction. The single element microstrip antenna has a very broad radiation pattern, which indicates that the antenna's gain will be poor; hence, it does not meet the objective of high gain >12dB for 5G applications. [29]. As a result, an antenna array is constructed and presented in order to improve the gain of the microstrip antenna.

The antenna array is a grouping of several small antennas which are joined to serve as a single antenna. The array elements are not necessarily identical but are preferred to have easier fabrication. Different kinds of antenna arrays exist based on the physical dispersion of the single elements. The famous types are shown in the Figure 4.1 [30]. Many parameters affect the antenna array's overall performance, which is determined in this chapter.

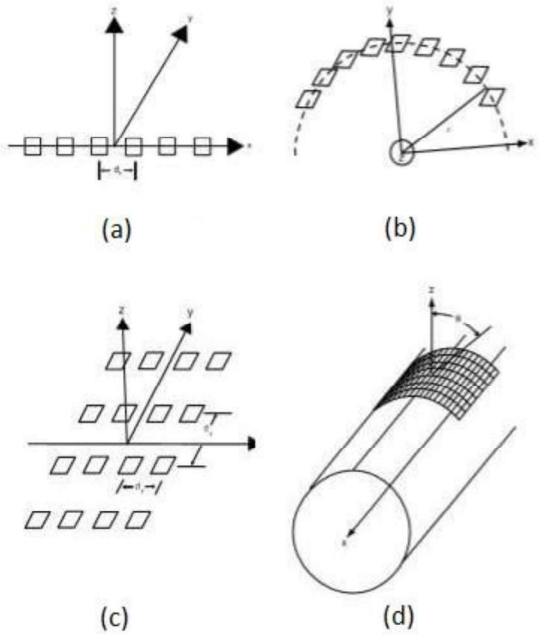

Figure 4.1 Antenna array types: (a) Linear array, (b) Circular array, (c) Planer array, and (d) Conformal array [30].

This chapter starts with a brief analysis of the feeding techniques. Then, a study of the distance between adjacent elements is presented. Finally, the simulation results of several planar dual-polarized aperture-coupled antenna arrays are presented.

4.1 Antenna array feeding Techniques

4.1.1 Series Feed

In a series feed design, the single elements are organized linearly and fed serially by a single transmission line where each patch feed from the previous one. Thus, every change to any patch has an instantaneous effect on the performance of the others.

The series feed has the lowest insertion loss but generally has the least polarization control and within the patches, the line's bandwidth is at its narrowest; thus, the phase between nearby components depends not only on line length but also on the input impedances of the patches.

Since the patches are amplitude-weighted with variable input impedances, the phases will be distinct for each element and will vary more radically when the frequency varies owing to the patch's narrowband nature [31].

Figure 4.2 shows the series feed which can be use in linear and planer antenna arrays.

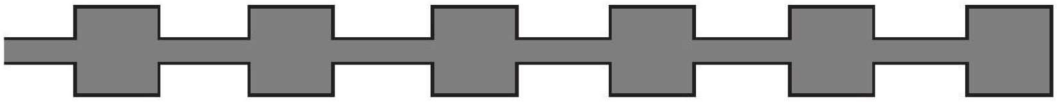

Figure 4.2 Series feed microstrip array.

4.1.2 Parallel Feed

The parallel feed, also called the corporate feed [32], consists of a branching network of two-way power dividers, as shown in Figure 4.3. Each branch divides again until it reaches the patch elements, which gives power splits of 2^n (where n is the number of distribution stages). In parallel feeds, the phase and magnitude of every element of the array can be manipulated since the feeding line lengths can be altered independently.

The most significant advantage of the parallel-fed microstrip antenna is the broadband bandwidth. There are two things that restrict the bandwidth of a parallel-fed microstrip array: the bandwidth of the patch element and the impedance matching circuit of the power-dividing transmission lines, such as the quarter-wave transformer. A series-fed array may obtain 1% or less bandwidth, but a parallel-fed array can get 15% bandwidth [31].

The disadvantage of parallel feed is that it requires long transmission lines between the input port and radiating elements; this causes a significant insertion loss value, thereby reducing the overall efficiency of the array [33].

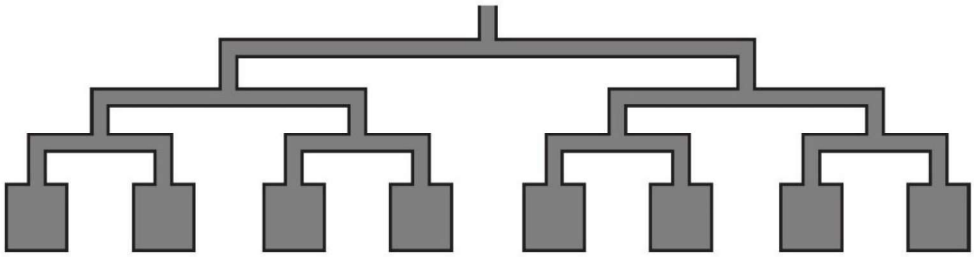

Figure 4.3 Parallel feed microstrip array.

4.1.3 Series - Parallel Feeding

The series-parallel feed consists of a combination of series and parallel-feed lines. The series-parallel feed has both advantages and disadvantages of series-feed and parallel-feed. The smaller series-fed subarray has a wider beamwidth and will suffer only a little loss of gain as a result of beam squint caused by a change in frequency. Hence, A series-parallel feed array with the same aperture size will produce a greater bandwidth than a series-fed array. Likewise, due to the partly parallel feed, the insertion loss of a series-parallel feed array is greater than that of a series-feed array. [31]. Figure 4.4 shows examples of different configuration of series-parallel feed techniques.

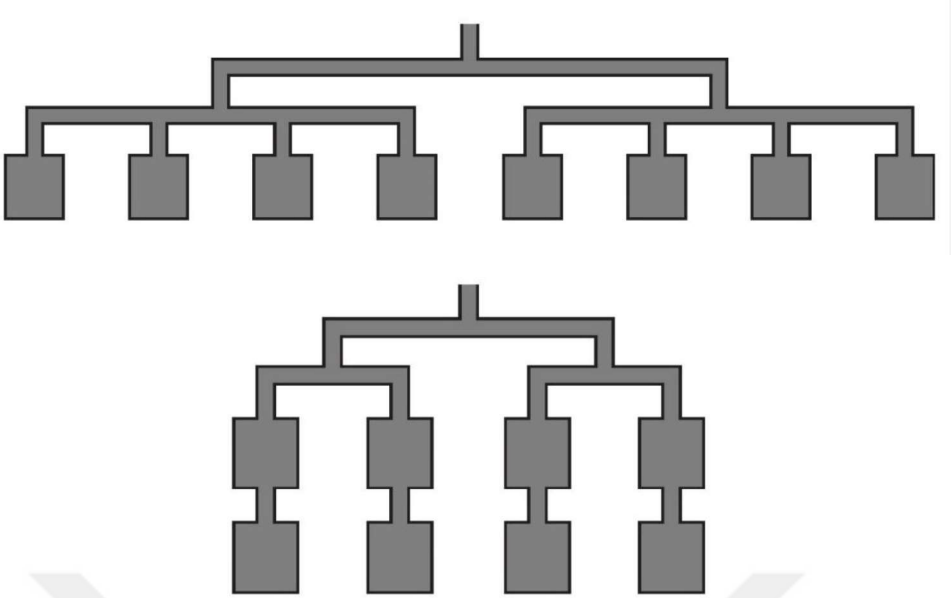

Figure 4.4 Parallel feed microstrip array.

4.2 The Distance between Single elements

One of the goals of 5G antenna array design is to maximize scanning angle while minimizing grating lobes. This is possible if the distance between the single element is less than half the wavelength according to (4.1).

$$d < \frac{\lambda}{1 + |\cos \theta_\circ|} \tag{4.1}$$

The goal here is to obtain 180° scanning angles, this can be achieved when $\theta_\circ = 0$, and $\cos 0 = 1$ which results in $d < 0.5\,\lambda$. This small distance between adjacent elements can cause an increase in the undesired mutual coupling. This affects the current distribution and, by extension, the input impedance and isolation between two single elements. Figure 4.5 shows infinite array geometry for linear and planar antenna array.

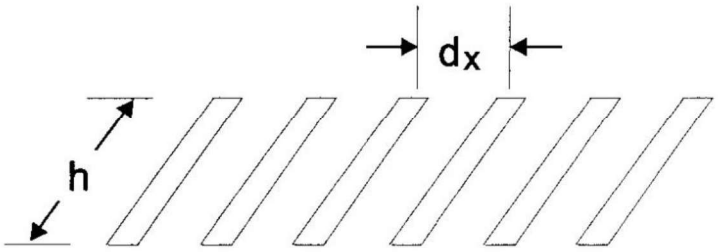

(a)

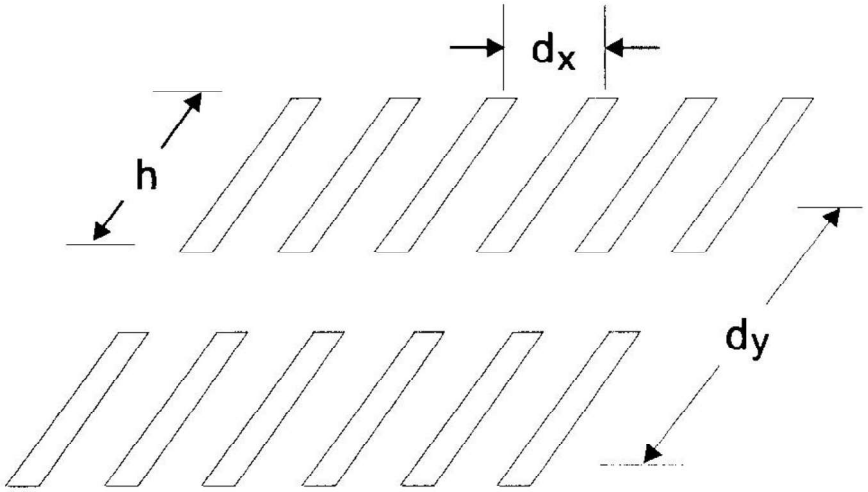

(b)

Figure 4.5 Infinite array geometries (a) linear antenna array, and (b) planer antenna array [34].

The space influence between two single elements was studied, Different values of inter-element space from center to center were used, where the antenna width/length is equal 61.93mm and the width of the feeder is 1.2 mm. Figure 4.6 shown the two single element of the array.

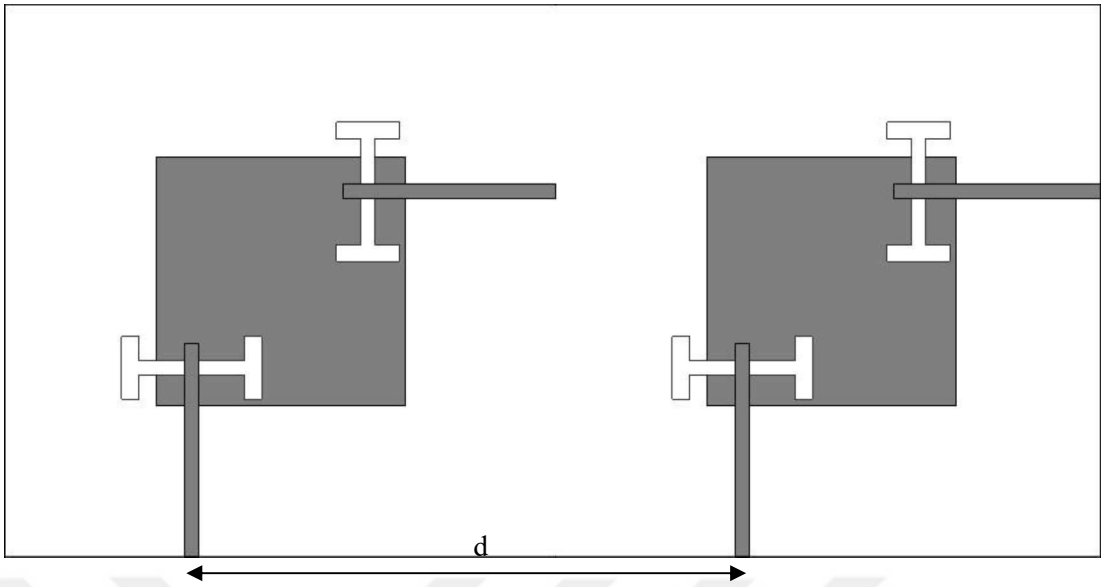

Figure 4.6 Two single element microstrip antenna.

Table 4.1 Inter-element space impact on the isolation between element and the realized gain.

Physical Space (mm)	Physical Space (λ)	S13 (dB)	S24 (dB)	Realized Gain (dB)
47.14	0.55 λ	-13.5	-20.6	9.82
51.42	0.6 λ	-15.35	-20.8	10.35
55.71	0.65 λ	-17.6	-22.4	10.67
59.99	0.7 λ	-19.54	-23.9	10.97
61.93	0.72 λ	-20.2	-24.5	11.08
64.28	0.75 λ	-21.9	-26.0	11.37
68.56	0.8 λ	-24.1	-27.6	11.53
77.13	0.9 λ	-27.6	-29.6	11.70
85.71	λ	-30.55	-30.7	11.68

It can be noted from Table 4.1 that as space increases, the isolation between the single elements decreases S13 and S42, respectively. Generally, it is acceptable at values lower than -20 dB; this value satisfies when space equal 0.70 λ. On the other hand, as the space increases, the realized gain will increase until it reaches a certain space, then it stops increasing, which is what we notice when a space equal λ.

4.3 2x2 antenna array design

This section presents a 2x2 dual-polarized planar antenna array. The configuration of the array is based on the single-element design shown in Figure 3.6. parallel feed

technique was used to connect between the single elements. Some bridges have been added in the port number 2 to overcome the interference between the two ports so that it does not affect their performance. The 2x2 antenna array is shown in Figure 4.7. the quarter-wavelength transformer was used to achieve the matching. Table 4.2 Presented are the values of the transmission lines in the feeding network. all the transmission line parameters were initially calculated using Macros tool in CST 2019 studio suite.

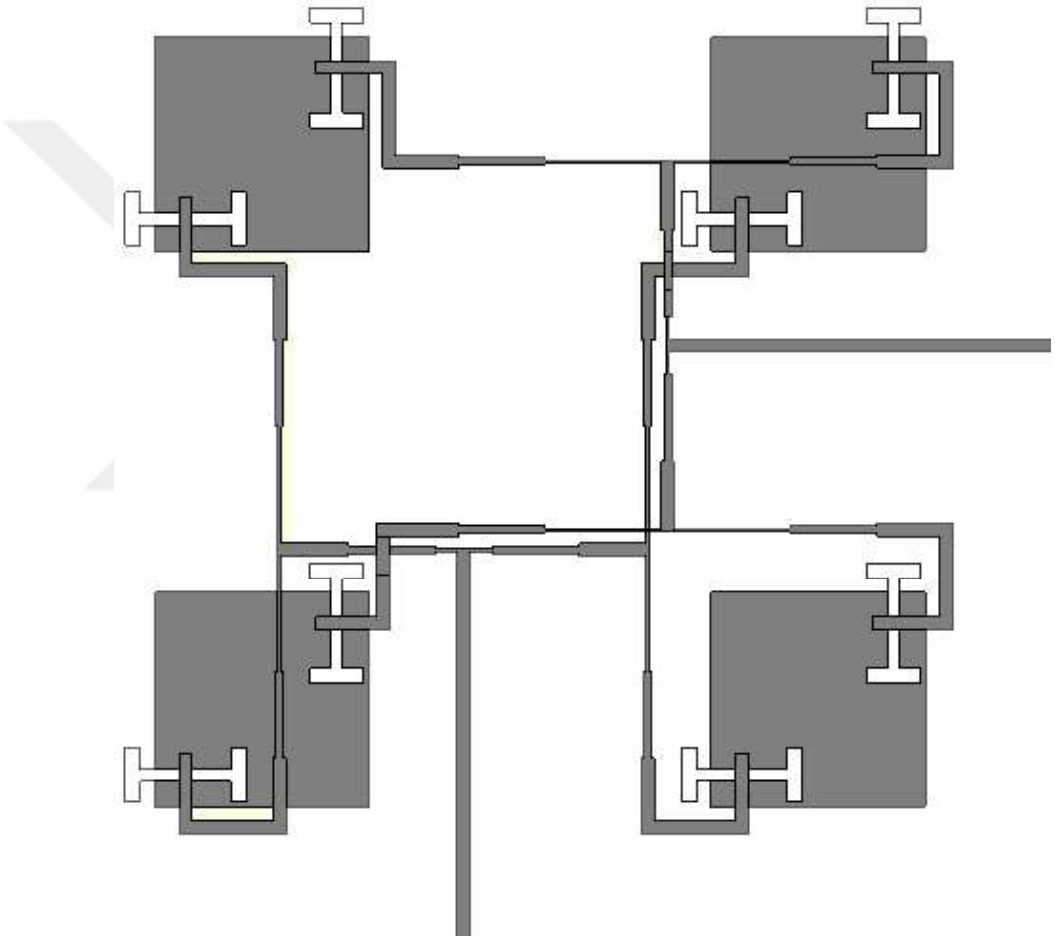

Figure 4.7 2x2 dual-polarized H-shaped aperture coupled microstrip antenna array structure (top view).

Table 4.2 Optimized parameters of the 2x2 dual-polarized Aperture Coupled microstrip antenna array.

Design Parameter	Description	Value (mm)
s	Space between the single elements	72.85
Wf50	Width of the 50Ω transmission line	1.68
Wf70	Width of the 70Ω transmission line	0.99
Wf100	Width of the 100Ω transmission line	0.45
lf50	Length of the long 50Ω transmission line	9
lf70	Length of the long 70Ω transmission line	11.37
lf100	Length of the long 100Ω transmission line	16.055
lff50	Length of the short 50Ω transmission line	9
lff70	Length of the short 70Ω transmission line	11.37
lff100	Length of the short 100Ω transmission line	3.735
wff	Microstrip feed line width	1.68
lff	Microstrip feed line length	50.735

After optimizing the array's feed network dimensions, the simulated return loss of the dual-polarized array has an S11 and S22 <-10 dB between 3.21-3.88GHz presented in Figure 4.8. it can be observed from Figure 4.9 that the simulated 2x2 antenna array isolation is better than 19 dB. The simulated gain of the array is presented in Figure 4.10. the array has a maximum gain of 13.84 dB in Port 1 and 13.62 dB in Port 2.

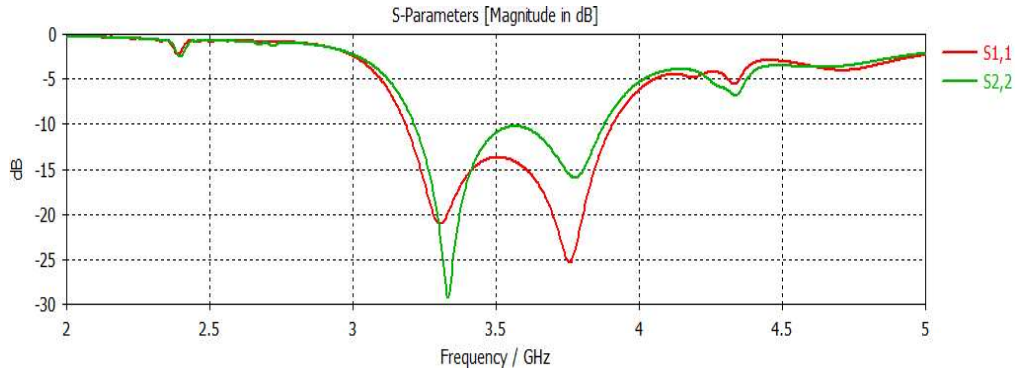

Figure 4.8 Simulation result of return loss S11 and S22 for 2x2 antenna array.

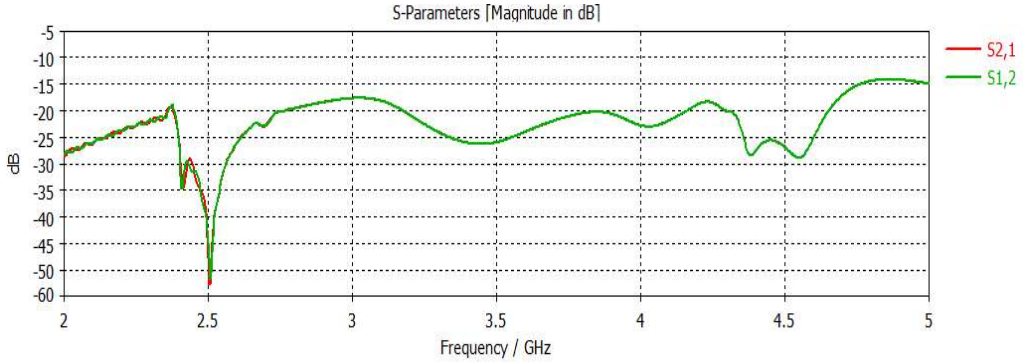

Figure 4.9 Simulation result of isolation between port S12 and S21 for 2x2 antenna array.

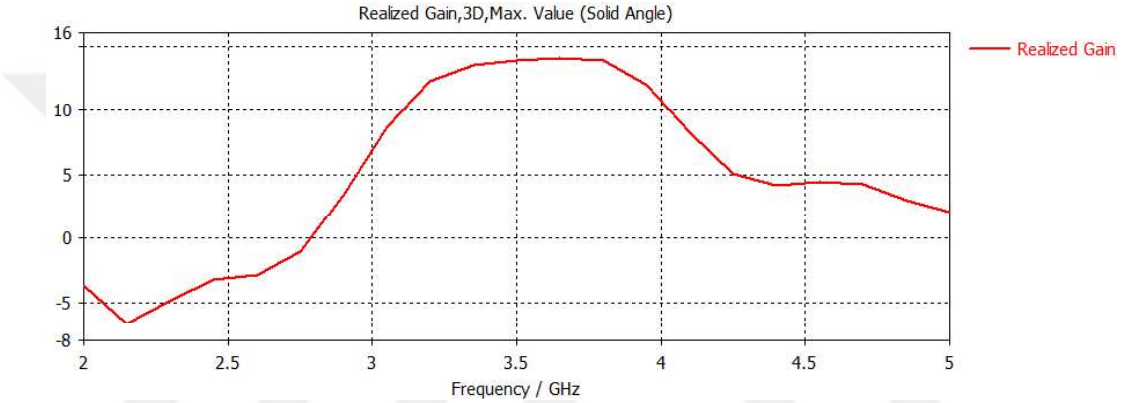

Figure 4.10 Simulated gain vs frequency for 2x2 dual-polarized antenna array.

As shown in Figure 4.11 and Figure 4.12, the normalized co-polarization and cross-polarization radiation patterns are simulated and evaluated for both the horizontal plane (xz-plane) and the vertical plane (yz-plane). Figure 4.13 presents 3D radiation patterns of the array. The array has a half power beamwidth (HPBW) of 29.9 degree and 31.3 degree, respectively.

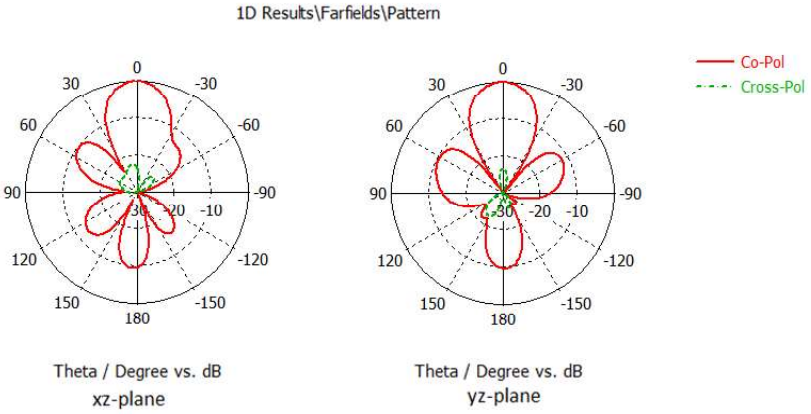

Figure 4.11 Radiation pattern of 2x2 antenna array for port1.

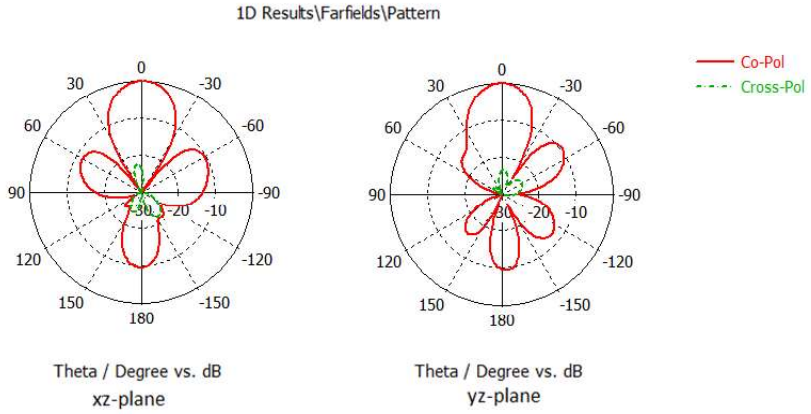

Figure 4.12 Radiation pattern of 2x2 antenna array for port2.

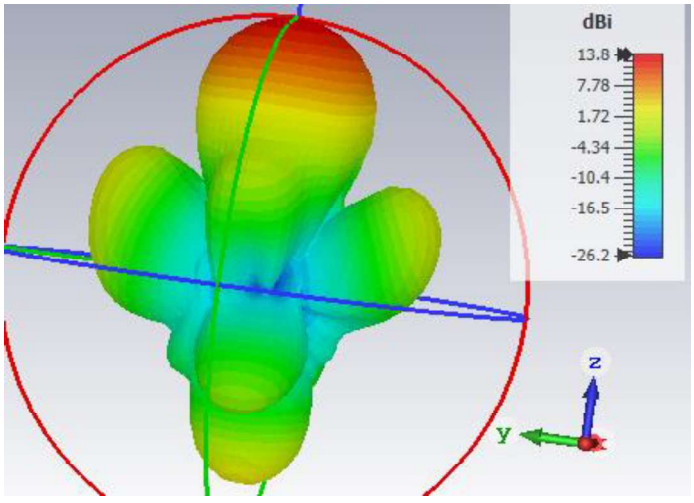

(a)